HHS Public Access

Author manuscript

Exp Neurol. Author manuscript; available in PMC 2024 August 25.

Published in final edited form as:

Exp Neurol. 2022 August ; 354: 114089. doi:10.1016/j.expneurol.2022.114089.

Oscillatory waveform sharpness asymmetry changes in motor thalamus and motor cortex in a rat model of Parkinson's disease

Louise C. Parr-Brownlie[a,b,*], **Christy A. Itoga**[b], **Judith R. Walters**[b], **Conor F. Underwood**[a]

[a]Department of Anatomy, Brain Health Research Centre, Brain Research New Zealand, University of Otago, Dunedin, New Zealand

[b]Neurophysiological Pharmacology Section, National Institute of Neurological Disorders and Stroke, National Institutes of Health, 35 Convent Drive, Building 35 Room 1C 903, Bethesda, MD 20892-3702, USA

Abstract

Parkinson's disease (PD) causes bursty and oscillatory activity in basal ganglia output that is thought to contribute to movement deficits through impact on motor thalamus and motor cortex (MCx). We examined the effect of dopamine loss on motor thalamus and motor cortex activity by recording neuronal and LFP activities in ventroanterior-ventrolateral (VAVL) thalamus and MCx in urethane-anesthetised control and parkinsonian rats. Dopamine lesion decreased the firing rate and increased the bursting of putative pyramidal neurons in layer V, but not layer VI, of the MCx without changing other aspects of firing pattern. In contrast, dopamine lesion did not affect VAVL firing rate, pattern or low threshold calcium spike bursts. Slow-wave (~1 Hz) oscillations in LFP recordings were analyzed with conventional power and waveform shape analyses. While dopamine lesion did not influence total power, it was consistently associated with an increase in oscillatory waveform sharpness asymmetry (i.e., sharper troughs vs. peaks) in both motor thalamus and MCx. Furthermore, we found that measures of sharpness asymmetry were positively correlated in paired motor thalamus-MCx recordings, and that correlation coefficients were larger in dopamine lesioned rats. These data support the idea that dysfunctional MCx activity in parkinsonism emerges from subsets of cell groups (e.g. layer V pyramidal neurons) and is evident in the shape but not absolute power of slow-wave oscillations. Hypoactive layer V pyramidal neuron firing in dopamine lesioned rats is unlikely to be driven by VAVL thalamus and may, therefore, reflect the loss of mesocortical dopaminergic afferents and/or changes in intrinsic excitability.

Keywords

Low threshold calcium spike (LTS) bursts; Basal ganglia; Slow wave oscillations; Dopamine; Motor thalamus; Motor cortex; Parkinson's disease

*Corresponding author at: Department of Anatomy, University of Otago, PO Box 913, Dunedin 9054, New Zealand. louise.parr-brownlie@otago.ac.nz (L.C. Parr-Brownlie).

Declaration of Competing Interest

The authors have no competing interests to declare.

1. Introduction

Animal models of Parkinson's disease (PD) show that loss of dopamine is associated with profoundly bursty and oscillatory neuronal activity in basal ganglia output. As a primary target of basal ganglia output, thalamocortical motor loops are hypothesized to be disrupted and underlie motor deficits in PD patients (Albin et al., 1989; Alexander and Crutcher, 1990; DeLong, 1990; DeLong and Wichmann, 2007; Bosch-Bouju et al., 2013), through improper motor program selection (Sommer, 2003) or decreased movement vigor (Thura and Cisek, 2017; Magnusson and Leventhal, 2021). Despite this, relatively few studies have examined dopamine lesion-induced changes in neuronal activity in the motor cortex (MCx) or motor thalamus (Mthal).

MCx neurons integrate diverse motor-related signals to optimize movement outcomes. During movements, the majority of MCx neurons modulate their activity (Levy et al., 2020) and populations of MCx neurons *briefly* synchronize changes in firing rate and pattern before messages descend the spinal cord (Evarts, 1966; Bauswein et al., 1989; Turner and DeLong, 2000; Saiki et al., 2018). MCx firing dynamics are altered in parkinsonian animals (Gross et al., 1983; Watts and Mandir, 1992; Goldberg et al., 2002; Parr-Brownlie and Hyland, 2005; Pasquereau and Turner, 2011; Pasquereau et al., 2016; Hyland et al., 2019; Rios et al., 2019). Oscillatory MCx activity, present in electroencephalography (EEG) and local field potential (LFP) signals, is also altered in PD. Traditional analysis of oscillatory MCx activity in the frequency-domain with Fourier-based methods have shown power differences, particularly in the beta-early gamma range, in PD, albeit more consistently in animal models (Sharott et al., 2005; Degos et al., 2009; Brazhnik et al., 2012; Jávor-Duray et al., 2015; Jávor-Duray et al., 2017; Brazhnik et al., 2021) than in patients (Hammond et al., 2007; de Hemptinne et al., 2013; Boon et al., 2019; Shirahige et al., 2020). More recently, analysis of MCx beta oscillations in the time-domain has uncovered asymmetrical (i.e. non-sinusoidal) differences in waveform shape in PD patients that track disease-severity and are modulated by dopaminergic therapy and deep brain stimulation (Cole et al., 2017; Jackson et al., 2019; O'Keeffe et al., 2020). Non-sinusoidal features of oscillatory waveforms are thought to reflect near-simultaneous bursts of synaptic activity and may, therefore, be a biomarker reflecting the degree of local synchrony (Sherman et al., 2016).

The Mthal comprises a group of ventral thalamic nuclei (ventroanterior [VA], ventromedial [VM] and ventrolateral [VL] thalamus) that receive afferents from basal ganglia or cerebellum (Ilinsky and Kultas-Ilinsky, 2001; Krack et al., 2002; Bosch-Bouju et al., 2013). Mthal neurons are modulated prior to or during movement (Strick, 1976; Schmied et al., 1979; Horne and Porter, 1980; Macpherson et al., 1980; Schlag-Rey and Schlag, 1984; Anderson and Turner, 1991; Nambu et al., 1991; Butler et al., 1992; Forlano et al., 1993; Butler et al., 1996; Inase et al., 1996; Raeva et al., 1999; Ivanusic et al., 2005; Kurata, 2005; Kunimatsu and Tanaka, 2010; Gaidica et al., 2018; Tanaka et al., 2018; Sauerbrei et al., 2020) and are essential for initiating goal-directed movements (Dacre et al., 2021; Takahashi et al., 2021), potentially by increasing the gain and bursting of layer V pyramidal neurons (Larkum et al., 2004; Park et al., 2020). Accordingly, Mthal occupies a central position in early (Albin et al., 1989; Alexander and Crutcher, 1990; DeLong, 1990; DeLong and Wichmann, 2007) and more recent (Bosch-Bouju et al., 2013; Magnusson and

Leventhal, 2021) theories linking neurophysiological changes in basal ganglia nuclei with the movement deficits of PD. Yet, there is currently no consensus regarding Mthal activity following dopaminergic lesion, with some studies reporting either no change, decreases or increases in firing rate at rest in the anesthetized or akinetic state (Voloshin et al., 1994; Schneider and Rothblat, 1996; Pessiglione et al., 2005; Kammermeier et al., 2016; Di Giovanni et al., 2020), while another reported specific changes in rate and bursts during movement execution (Bosch-Bouju et al., 2014).

Currently, there is uncertainty surrounding the precise changes in Mthal and MCx activity in the dopamine-depleted state that is hampering full characterization of parkinsonian pathophysiology. To resolve this, we sought to characterize spike and LFP activities of MCx, Mthal and MCx-Mthal interactions in unilateral 6-hydroxydopamine (6-OHDA) lesioned rats under urethane anesthesia, which presents a stable brain state free of behavioral confounds where the effects of dopamine loss on inputs from basal ganglia are well described (Vila et al., 2000; Magill et al., 2001a; Parr-Brownlie et al., 2007; Walters et al., 2007). To characterize dopamine lesion-induced changes in MCx and Mthal, data were compared between naïve control rats and the lesioned and contralateral (non-lesioned) hemisphere in unilaterally lesioned rats.

2. Methods

All experimental procedures were conducted on male Sprague-Dawley rats (Taconic Farm, U.S.A.) in accordance with the NIH Guide for Care and Use of Laboratory Animals and were approved by the NINDS Animal Care and Use Committee. Rats were housed with ad libitum access to chow and water in environmentally controlled conditions. Every effort was made to minimize the number of animals used.

2.1. Unilateral 6-hydroxydopamine lesion procedure and behavioral testing

Unilateral lesions were performed on rats weighing 270–350 g at the time of lesion surgery. Rats were anesthetized with ketamine (100 mg/kg, i.p., Ketaved, Vedco Inc., U.S.A.) and xylazine (10 mg/kg, i.p., AnaSed, Lloyd Laboratories, U.S.A.), the incision area was shaved and a long acting local anesthetic (1% mepivacaine HCl solution s.c., Astra-Zeneca, U.S.A.) was injected along the intended incision line. Rats were injected with desmethylimipramine (15 mg/kg i.p., Sigma-Aldrich, U.S. A.) 30 min prior to the neurotoxic lesion. The rat was mounted in a stereotaxic frame (David Kopf Instruments, U.S.A.), and ophthalmic ointment (Puralube, Fougera & Co, U.S.A.) was applied to the eyes to prevent corneal dehydration. The skull was exposed by a midline sagittal incision, a hole was drilled above the left medial forebrain bundle and the dura was reflected. Target coordinates for the cannula were centered at anteroposterior (AP) +4.4 mm from the lambdoid suture and lateral −1.2 mm from lambda in the flat skull position and the cannula was lowered 8.3 mm from the skull surface. A solution containing 6 μg of 6-hydroxydopamine HBr (6-OHDA) in 3 μL of 0.9% saline solution containing 0.008% ascorbic acid (Sigma-Aldrich) was infused at 1 μL/min via a cannula into the medial forebrain bundle. Following the infusion, the cannula remained at the target site for an additional 3 min to prevent diffusion of the neurotoxin. Body temperature was maintained at 36–38 °C throughout the procedure by a heating pad.

The post-operative diet of lesioned rats was supplemented with fruit and gelatin to maintain normal weight.

The extent of the dopaminergic denervation was tested behaviorally 5–7 days after the lesion using the step test (Olsson et al., 1995). Only rats that demonstrated a strong lesion effect (number of steps by contralateral limb/number of steps by ipsilateral limb <5%) were used for electrophysiological recordings. Studies in our lab (Parr-Brownlie et al., 2007) and others (Olsson et al., 1995; Tseng et al., 2005) have shown that severely impaired stepping behavior is associated with more than 95% of dopamine depleted in the ipsilateral striatum or loss of more than 95% of dopamine neurons in the ipsilateral substantia nigra pars compacta.

2.2. Single unit and local field potential (LFP) recording procedures

Extracellular single-unit and LFP recordings were conducted in the MCx and/or Mthal 7–13 days after unilateral 6-OHDA infusion. A total of $n = 68$ rats were used for electrophysiological recordings, comprising $n = 54$ 6-OHDA lesioned rats and $n = 14$ naïve control rats. Neuronal activity was recorded from both VA and VL (VAVL) Mthal nuclei because they innervate the MCx, whereas VM Mthal connects to the associative cerebral cortex (Cicirata et al., 1986; Aldes, 1988; Rouiller et al., 1993; Rajakumar et al., 1994; Gerfen and Wilson, 1996; Wang and Kurata, 1998; Bosch-Bouju et al., 2013). Anatomical data show that that VA and VM Mthal receive inputs from the basal ganglia output nuclei, suggesting that they might be more affected by loss of dopamine (Anderson and DeVito, 1987; Sakai et al., 1996; Kuramoto et al., 2011). However, movement-related activity is very similar between VA (basal ganglia-receiving) and VL (cerebellar-receiving) nuclei (Anderson and Turner, 1991; Nambu et al., 1991; Bosch-Bouju et al., 2014) and also similarly affected after dopamine lesion (Bosch-Bouju et al., 2014), possibly because both areas receive inputs from MCx and reticular thalamus (Paŕe et al., 1987; Hazrati and Parent, 1991; Sakai et al., 2000; McFarland and Haber, 2002) and there is a small area in anterior VL that receives both basal ganglia and cerebellar inputs (Percheron et al., 1996; Sakai et al., 1996). In this study, lesioned and non-lesioned (NL) hemispheres refer to ipsilateral and contralateral to 6-OHDA infusion, respectively. Single-units and LFPs were also recorded in control (neurologically intact) rats weighing 230–390 g at the time of surgery. In some experiments, pairs of VAVL-MCx neurons were simultaneously recorded to examine firing relationships in the thalamocortical pathway.

All recordings were conducted under urethane anesthesia (1.4 g/kg i.p. with additional doses as needed, Sigma-Aldrich). Rats' heads, right axilla and left pelvic regions were shaved, mepivacaine HCl solution was injected s.c. along the intended incision line on the head, surface electrocardiogram (ECG) electrodes were placed in the axilla and pelvic regions (Lead II, Grass, U.S.A.) and ophthalmic ointment was applied to the eyes. Rats were placed in a stereotaxic frame with a heating pad to maintain body temperature and a force sensing resistor (Interlink Electronics, U.S.A.) was placed under the diaphragm region. ECG and respiration were monitored to ensure the animals' wellbeing. Craniotomies were made over target coordinates, relative to bregma (flat skull position) for MCx (AP +2.0 mm, lateral ±2.2 mm) or VAVL (AP −2.1 mm, lateral ±1.8 mm).

Glass microelectrodes with impedances of 4–7 MΩ (measured at 135 Hz, tip diameter 1–2 μm) were used to record extracellular action potentials and LFPs. Glass electrodes were filled with 1% Pontamine Sky Blue dye in 2 M NaCl solution. Electrodes were lowered into the brain until they were just above the target structures and advanced slowly using hydraulic microdrives (Narishige International USA Inc.) to isolate single cells (dorsoventral from the dura: MCx 0.5–3.0 mm; VAVL 5.4–6.5 mm; SNpr 7.6–9.0 mm). Sampling rates were 27 and 1 kHz for unit and LFP activities, respectively (Micro 1401, Cambridge Electronic Design, U.K.). Action potentials were amplified (3000×), bandpass filtered (250–5000 Hz) and monitored on oscilloscopes (Hewlett-Packard, Palo Alto, CA, U.S.A.) and audiomonitors (Grass). LFPs were amplified (2000×) and bandpass filtered (0.1–100 Hz). Discriminated signals were digitized, stored and analyzed using Spike2 data acquisition and analysis software (Cambridge Electronic Design). Neuronal spike trains were recorded for at least 7 min.

2.3. Data analysis

For analyses of spontaneous activity, one 300 s epoch of simultaneously recorded spiking and LFP activities that was free of artifacts was used from every recorded neuron. Data are represented as means ± standard error of the means (SEM).

Oscillatory characteristics of spike train activity were analyzed by the method of Kaneoke and Vitek (1996). Briefly, a Lomb periodogram based analysis was performed on spike train autocorrelograms (50 ms bins, 10 s lag). For evenly sampled data, the Lomb algorithm is similar to a fast Fourier transform (FFT) (Shrager, 2003). Periodogram spectra were used to determine frequencies with power significantly ($p < 0.05$) greater than expected in comparison with independent Gaussian random values. Firing rate was calculated from the mean interspike interval (ISI) and spike train regularity was determined using ISI coefficient of variation (ISI CV).

Two types of “burst analyses” were conducted on recorded data. First, spike train burstiness was assessed in all recorded spike trains by the density discharge histogram method as described previously (Kaneoke and Vitek, 1996; Parr-Brownlie et al., 2007; Walters et al., 2007; Bosch-Bouju et al., 2014). This analysis defines a burst as a period of time where there are significantly more spikes compared to other periods in the spike train, and was used to categorize the general firing pattern of the spike train. A burstiness index ≥0.5 was used for this analysis, so that the bin width of the discharge density histogram was twice the mean interspike interval (ISI). A spike train was classified as bursty if it met the following criteria: the distribution of its discharge density histogram was significantly different from a Poisson distribution of the discharge density histogram (chi square test set at a significance level of 0.05), the histogram was positively skewed, there were at least 3 spikes in the burst, firing rate was higher than 1.0 Hz and the number of bursts/1000 spikes was >5. For MCx neurons, firing rate was not a criterion to determine bursts because firing rate is low in this population and affected by 6-OHDA lesion. Second, the characteristics of low threshold calcium spike (LTS) bursts were examined in only VAVL spike trains. These spike bursts are a feature of thalamic neurons in anesthetized, sleeping and moving animals, and are caused by deinactivation of transient calcium channels following sustained hyperpolarization of

thalamic membrane potential (Llinas and Jahnsen, 1982; Jahnsen and Llinas, 1984; Steriade et al., 1990a; Bosch-Bouju et al., 2014). These very high frequency bursts are presumed to facilitate synaptic reliability (Bosch-Bouju et al., 2013). The criteria used to define LTS bursts were: the first ISI in the burst was ≤5 ms, subsequent ISIs in the bursts were ≤ 7 ms, and the burst was preceded with a silent period of at least 100 ms (Jahnsen and Llinas, 1984; Steriade et al., 1985; Steriade et al., 1990a; Lacey et al., 2007; Parr-Brownlie et al., 2009; Bosch-Bouju et al., 2014; Nakamura et al., 2014). LTS bursts contained 2–8 spikes.

We performed FFT power and waveform shape analysis on multiple LFPs for each rat (one LFP per electrode track) and then averaged the data to give a single data point per rat. For both types of LFP analysis, LFP signals were down-sampled to 20 Hz and high pass filtered at 0.2 Hz (Spike2). LFP power was calculated using FFT with 256 blocks and a measure of total power was obtained by summing the area of individual 0.078 Hz bins over the 0.3–2.5 Hz range from 300 s epochs of data.

Waveform shape analyses were performed using the method of Cole et al. (2017), adapted for the dominant ~1 Hz oscillation present under urethane anesthesia. Down-sampled MCx and VAVL LFPs were first cleaned of high-frequency oscillations that would interfere with accurate detection of peaks and troughs by applying a 6 Hz low-pass FIR filter. All measurements were performed on this trace. To detect waveform extrema, the trace was duplicated and band-pass filtered at 0.3–1.2 Hz and the minimum (for troughs) or maximum (for peaks) voltage between two consecutive zero-crossings was determined. Extrema sharpness was calculated as the mean of the difference in voltage between the extrema and 50 ms before and after it. Peak and trough sharpness were measured for all cycles in the 300 s epoch and averaged. To account for differences in LFP amplitude across recordings, the sharpness ratio was computed by taking a ratio of the epoch-averaged peak and trough sharpness (or the inverse if the result is <1). Rise and decay steepness were determined by measuring the slope between a trough and subsequent peak or peak and subsequent trough, respectively. Steepness ratio was calculated as the maximum ratio of epoch-averaged rise and trough steepness. A Spearman's correlation was performed for each LFP recording to ascertain the relationship between waveform sharpness and amplitude. For this analysis, sharpness ratio was calculated for each cycle and compared with the peak-to-trough amplitude of the same cycle. Since individual cycles within a LFP are not independent, the statistical significance of correlations for individual LFPs was not determined. Instead, we tested the hypothesis that correlation coefficients for all LFPs recorded in each group differed from zero with a one sample *t*-test (Cole et al., 2017).

The relationships between simultaneously recorded spike trains from VAVL-MCx were evaluated with cross correlograms constructed from 300 s epochs using Spike2 analysis software (5 ms bins, 8 s lag) with the MCx spike train used as the reference spike (time zero). To assess the significance of the correlation in firing pattern between each pair of neurons, a baseline firing rate was determined over the first or last 0.5 s of the cross-correlogram, whichever had the largest standard deviation (SD). Thresholds were defined as the baseline ±3SD. If at least three consecutive bins of the cross-correlogram exceeded the threshold, the neuron pair was classified as correlated. For correlated pairs, the time

between peak activity in the VAVL neuron with respect to the MCx neuron was measured on correlograms with smoothed (cubic spline) bins.

Action potential widths of neurons recorded in layers II/III, V and VI of MCx were measured for the purpose of categorizing cells as having either ‘broad’ (putative pyramidal neurons) or ‘narrow’ (putative interneurons) waveforms. For each neuron, the time (ms) between the first peak and trough of the mean action potential was measured (indicated by the arrowheads in Fig. 1), regardless of the order in which they occurred (Wilson et al., 1994; Parr-Brownlie and Hyland, 2005). Previous studies comparing electrophysiological characteristics with neuron morphology in the cortex have reported that neurons can be reliably distinguished based on action potential width; the width is larger for pyramidal neurons than interneurons (Tierney et al., 2004; Tseng et al., 2006). Although previous studies have measured different parts of the action potential, affecting the absolute value of action potential width used to separate pyramidal neurons and interneurons, studies consistently report a bimodal distribution of action potential width (Rao et al., 1999; Constantinidis and Goldman-Rakic, 2002; Bartho et al., 2004; Tierney et al., 2004; Tseng et al., 2006; Parr-Brownlie et al., 2007). Fig. 1 shows a histogram of mean action potential width from 182 neurons recorded in the MCx. Lines representing the weighted sum of one, two or three Gaussian curves were fitted to the histogram using SigmaPlot (Systat Software, San Jose, CA, U.S.A.). The line of two Gaussian curves best fitted ($r^2 = 0.84$) the distribution. Further examination of the bimodal distribution showed that there was overlap of the two individual Gaussian curves, indicating that a subset of recorded neurons could belong to either the broad and narrow waveform groups. For this analysis, neurons with action potential waveforms that were outliers (mean - 2SD, i.e. <5% single tail) with respect to the Gaussian curve of broad waveforms were classified statistically as belonging to only the narrow group. Outliers for the Gaussian curve of narrow waveforms (mean + 2SD) were classified as having broad action potential widths. Action potential widths that statistically belonged to both individual Gaussians formed a third ‘intermediate’ waveform group (unfilled bars) that was analyzed separately from the narrow and broad groups. A waveform was classified as narrow if the action potential width was ≤0.347 ms, intermediate waveforms had widths between 0.348 and 0.399 ms, and broad waveforms had widths ≥0.400 ms. The majority of recorded neurons (137/183, 74.9%) had broad action potential waveforms, and 19.7% (36/183) and 5.4% (10/183) of recorded neurons had narrow and intermediate waveforms, respectively. The proportion of putative pyramidal neurons (broad action potentials) is consistent with other studies in the cortex (Winfield et al., 1980; Connors and Gutnick, 1990). The mean peak to trough widths for neurons with narrow, intermediate and broad action potential waveforms were 0.263 ± 0.007 ms, 0.372 ± 0.005 ms and 0.613 ± 0.011 ms, respectively, and representative narrow and broad waveforms are shown in Fig. 1.

The effects of lesion on firing rate, LTS bursts per spike train, and LFP power and shape were compared using a one factor analysis of variance (ANOVA) with Holm-Sidak post-hoc comparisons if the data were normally distributed or Kruskal-Wallis ANOVA with Dunn’s method post-hoc comparisons when the data were not normally distributed. We elected to use unpaired hypothesis tests, instead of less conservative paired tests, to compare non-lesioned and lesioned hemispheres because an unequal number of cells/LFPs were

recorded from each hemisphere in most rats. For VAVL-MCx paired recordings, significant differences in the latency of correlated spiking activity between the lesioned hemisphere and control rats was assessed using Mann Whitney *U* tests. ISIs in LTS bursts were analyzed by a 3-way ANOVA, with hemisphere (control, non-lesioned and lesioned), size of LTS bursts (doublets to quintuplets), and position of the ISI in LTS bursts (first ISI vs second ISI etc.) as factors. Post-hoc comparisons were made using Bonferroni's test. Incidences of spike trains with bursty activity, oscillatory activity, LTS bursts and correlated cross-correlograms were compared between hemispheres using chi square or Fisher's exact probability tests. Criterion for statistical significance was $p \leq 0.050$. For comparisons that reached statistical significance, we calculated the Hedges' g value as a standardized measure of effect size (Ho et al., 2019).

2.4. Histology

Following the completion of recordings, the last recording sites were marked by iontophoresis (−18 μA for 25 min) of Pontamine blue dye. After rats were sacrificed, brains were removed, frozen and 20 μm sections were cut on a cryostat. Slices containing the VAVL or MCx were stained with neutral red (FD NeuroTechnologies Inc.) to verify the site of the last recording. Sites of neurons recorded earlier in the experiment were reconstructed based on recording coordinates. Only neurons that were confirmed to be in the target structures were used for analyses. Recording sites in MCx and VAVL are shown in Fig. 2.

2.5. Quantitative measurement of dopamine

For quantitative assessment of the 6-OHDA lesion, control ($n = 6$) and 6-OHDA lesioned (n = 6) rats were anesthetized with chloral hydrate (400 mg/kg i.p., Sigma), decapitated and brains were rapidly frozen on dry ice. Micro-punch samples were collected from consecutive sections (300 μm) containing the striatum or MCx. Frozen tissue samples were weighed, homogenized and deproteinised using 400 μL solution containing 0.4 M perchloric acid (Sigma) and 0.5 mM EDTA (Sigma). Homogenates were centrifuged (16,000 rpm) and supernatants were stored at −80 °C. Dopamine in the supernatant was adsorbed onto alumina (MP Biomedicals, Irvine, CA, U.S.A) using Tris buffer (1.0 M Tris (MP Biomedicals) and 50 mM EDTA, pH adjusted to 8.6 using HCl), washed with milliQ water and desorbed using a solution containing 90% 0.2 M acetic acid (Sigma) and 10% 0.2 M orthophosphoric acid (Sigma). The extract (90 μL) was analyzed by reverse phase high performance liquid chromatography with electrochemical detection (HPLC-ED) as described previously (Eisenhofer et al., 1986). Dopamine amounts are expressed as pg of dopamine per mg of frozen tissue. Dopamine amounts were analyzed between control, non-lesioned and lesioned hemispheres using ANOVA with Holm-Sidak's method for *posthoc* testing. For each rat, the percentage of dopamine in the striatum or motor cortex was calculated by dividing the amount of dopamine in the left hemisphere by the amount in the right hemisphere. Differences in the percentage of dopamine between control and 6-OHDA lesioned rats were analyzed by *t*-tests with $p < 0.05$ level of significance.

3. Results

3.1. Effect of dopamine loss on putative pyramidal neuron spike train activity from MCx

To investigate whether dopamine cell lesion affected MCx activity in urethane anesthetized rats, MCx spike trains were examined from control rats (n = 56 cells recorded from 9 rats), and in non-lesioned (contralateral to 6-OHDA infusion, n = 51 cells from 26 rats) and dopamine lesioned hemispheres (n = 75 cells from 30 rats) 7–13 days after 6-OHDA infusion into the left medial forebrain bundle. Almost all recorded neurons (182/183, 99.5%) were from layers V and VI. The single neuron recorded in layer II/III was not used in any analyses of spike train activity. Neuronal recordings were further characterized into those that had broad and narrow action potential waveforms (see methods), indicative of putative pyramidal neurons and interneurons, respectively. Approximately 75% of recorded neurons were putative pyramidal neurons; 68% (38/56) in control rats, 80% (41/51) in non-lesioned and 76% (57/75) in lesioned hemispheres. Fig. 3A shows representative spike trains recorded from putative pyramidal neurons from control, non-lesioned and lesioned hemispheres.

Dopamine cell lesion was associated with a significant decrease in the firing rate of putative pyramidal neurons in the MCx when compared to control rats (1.2 ± 0.3 and 2.5 ± 0.5 spikes/s, respectively, p = 0.013; Hedges' g = 0.51). The firing rate of putative pyramidal neurons in the non-lesioned group (1.8 ± 0.6 spikes/s) did not differ from control rats or the lesioned hemisphere. Spontaneous firing rates of MCx neurons with broad action potentials were low (range in control rats = 0.04–14.1 spikes/s, median 0.9 spikes/s), and 53% (20/38) of the spike trains in control rats had firing rates <1.0 spike/s. Further analysis revealed that the lesion had a larger effect on neurons with broad action potentials in layer V than those in layer VI. When firing rate was compared for putative pyramidal neurons in layer VI, there were no significant differences between control (2.0 ± 0.6 Hz, n = 20 cells from 7 rats), non-lesioned (1.0 ± 0.2 Hz, n = 24 cells from 18 rats) and lesioned hemispheres (1.2 ± 0.3 Hz, n = 44 cells from 23 rats). In contrast, for putative pyramidal neurons in layer V, firing rate was significantly lower in the lesioned hemisphere (n = 13 cells from 8 rats) than in control rats (n = 18 cells from 6 rats, Fig. 3B, p = 0.003; Hedges' g = 0.99), while firing rate in the non-lesioned hemisphere (n = 17 cells from 9 rats) did not differ significantly from control or lesioned hemispheres.

Significant changes in putative neuron activity in the MCx may have arisen through reduced dopaminergic input to the MCx as a consequence of the 6-OHDA lesion. Mesocortical dopamine neurons innervate the MCx, although not as densely as other frontal cortex regions such as the anterior cingulate cortex (Lindvall and Bjorklund, 1974; Tassin et al., 1978). Lesion of dopamine neurons by injection of 6-OHDA into the medial forebrain bundle caused severe depletion of dopamine in the striatum and partial depletion in the MCx. Striatal dopamine content and percent loss have been reported previously (Parr-Brownlie et al., 2007); there was profound (99%) loss of striatal dopamine in 6-OHDA lesioned rats compared to control rats (n = 6 rats/group). Dopamine content (pg/mg tissue) in the lesioned MCx was significantly lower (14.9 ± 1.7, p = 0.032) than the MCx from control rats (27.8 ± 4.4; Hedges' g = 1.33) or the non-lesioned (23.8 ± 2.9; Hedges' g

= 1.20) hemisphere 7–8 days after unilateral injection of 6-OHDA. Accordingly, the inter-hemispheric difference in dopamine content (37%) was significantly ($p = 0.009$; Hedges' g = 1.29) larger in lesioned than control rats (Fig. 3C). The extent of dopamine loss in the MCx is consistent with previous studies reporting reduced (25–30%) dopamine levels or tyrosine hydroxylase-positive fibers in the MCx of rats following 6-OHDA lesion (Whishaw et al., 1992; Debeir et al., 2005; Guo et al., 2015) and in the MCx of Parkinson's patients (Gaspar et al., 1991).

Dopamine cell lesion induced changes in the firing pattern of MCx cells were subtle. There were no significant differences in the incidence of spike trains with oscillatory or bursty firing patterns or ISI CV in layers V or VI, therefore, data were pooled and the mean values across layers V and VI are presented. Approximately half (66/136, 48.5%) of the spike trains recorded in the MCx exhibited a firing pattern with significant oscillatory activity in the 0.3–2.5 Hz range as measured by spectral analysis of Lomb periodograms (Kaneoke and Vitek, 1996). Dopamine cell lesion did not alter the proportion of spike trains with oscillatory firing patterns (Fig. 3D). Spike train regularity, as measured by ISI CV, did not differ between spike trains recorded from putative pyramidal neurons in control rats, non-lesioned and lesioned hemispheres (Fig. 3E). The incidence of spike trains with a bursty firing pattern, assessed by the density histogram method (Kaneoke and Vitek, 1996), did not differ significantly between putative pyramidal neurons in control rats, non-lesioned and lesioned hemispheres (Fig. 3F). However, we did find that the mean burst rate of layer V neurons was significantly ($p = 0.009$; Hedges' g = 0.82) larger in the lesioned hemisphere than in the control hemisphere, although the contralateral non-lesioned hemisphere was not statistical different from the lesioned or control hemispheres (Fig. 3G). In contrast, the mean burst rate of layer VI neurons was similar ($p > 0.05$) between control rats (29.3 ± 7.4 bursts per 1000 spikes), non-lesioned (16.7 ± 5.2) and lesioned hemispheres (19.7 ± 4.5). Thus, while dopamine lesion did not influence the proportion of bursty cells in MCx, it did increase the burst rate of layer 5 neurons.

3.2. Effect of dopamine loss on MCx LFP activity

LFP activity was dominated by the ~1 Hz oscillatory activity indicative of urethane anesthesia (Fig. 4A). LFP measures did not differ between layers V or VI in the MCx so data were averaged across these layers. Analysis of MCx LFPs in the frequency-domain showed that FFT power in the 0.3–2.5 Hz range did not differ significantly between control ($n = 14$ rats), dopamine lesioned ($n = 43$ rats) and non-lesioned hemispheres ($n = 31$ rats, Fig. 4B).

In contrast to FFT analysis, analysis of MCx LFP waveform shape in the time-domain revealed clear differences in sharpness asymmetry between dopamine lesioned and control rats. This is illustrated by the degree of overlap in the histogram of peak and trough sharpness values for representative LFP recordings from control, non-lesioned and lesioned hemispheres (Fig. 4C). Sharpness asymmetry, quantified as the sharpness ratio (Fig. 4D), was significantly larger in lesioned ($p < 0.001$; Hedges' g = 1.33) and non-lesioned hemispheres ($p = 0.015$; Hedges' g = 1.02) relative to control rats. Consistent with reported findings in PD patients (Cole et al., 2017), we found that sharpness ratio was, on average,

positively correlated with peak to trough amplitude in LFPs recorded from control, non-lesioned and lesioned hemispheres (all $p < 0.0001$, one sample t-test; Fig. 4E). Interestingly, correlation coefficients were larger in lesioned hemisphere ($p = 0.002$; Hedges' g = 0.54) compared to control rats. We did not detect any differences between the hemispheres for steepness asymmetry (Fig. 4F).

3.3. Simultaneously recorded putative pyramidal neuron in MCx and VAVL neuron after dopamine loss

To examine the possibility that oscillations in MCx spike trains might be entrained by oscillatory activity in the basal ganglia-thalamocortical pathways, phase relationships between firing patterns of putative pyramidal MCx neurons and VAVL thalamus neurons were examined. VAVL, but not VM, was chosen because it provides the densest thalamic input to rat MCx (Cicirata et al., 1986; Aldes, 1988; Rouiller et al., 1993; Wang and Kurata, 1998). Spike trains and LFPs were simultaneously recorded from VAVL and MCx in control or dopamine lesioned hemispheres (Fig. 5A).

Cross-correlograms in Fig. 5B show examples of correlated activity between putative pyramidal neurons in MCx and VAVL neurons in control and dopamine lesioned hemispheres. Few (3/25, 12%) MCx-VAVL spike trains in the control hemisphere exhibited significantly correlated activity in cross-correlograms (Fig. 5B,C) and this measure was not affected by dopamine cell lesion ($n = 24$ paired recordings). All correlated cross-correlograms had an in-phase firing relationship, concordant with known reciprocal glutamatergic projections between MCx and VAVL thalamus. While VAVL neurons consistently fired before putative pyramidal neurons in MCx in control rats (3/3 correlated pairs), timing appeared to be more variable in the lesioned hemisphere with putative pyramidal neurons sometimes (2/4, 50%) firing after VAVL neurons. However, the mean difference in the timing of firing between putative pyramidal neurons in MCx and VAVL neurons was not statistically different between control rats and the 6-OHDA lesioned hemisphere (Fig. 5C). The relatively small population of MCx-VAVL neurons exhibiting in-phase correlated activity in control and PD model rats indicates that, under urethane anesthesia, dopamine loss does not affect the timing of spiking between these two motor areas.

3.4. Effect of dopamine loss on spike train activity in VAVL thalamus

VAVL thalamus is critically positioned to control the cortical-passage and expression of the profoundly bursty and oscillatory firing pattern observed in the dopamine-deficient basal ganglia output consistently reported in the urethane anesthetized state (Murer et al., 1997a; Belluscio et al., 2003a; Walters et al., 2007; Lobb and Jaeger, 2015). VAVL spike trains were analyzed to determine if VAVL activity was altered by dopamine cell lesion. Representative VAVL thalamus spike trains from control rats, and non-lesioned and lesioned hemispheres are shown in Fig. 6A.

Consistent with putative pyramidal neuron activity in layer VI of MCx, dopamine cell lesion did not alter VAVL spike train activity. VAVL firing rate did not differ between spike trains recorded in control ($n = 63$ from 10 rats), non-lesioned ($n = 60$ from 15 rats) and lesioned

(n = 66 from 17 rats) hemispheres (Fig. 6B). Dopamine cell lesion did not alter the number of spike trains in ipsilateral VAVL exhibiting oscillatory activity in the 0.3–2.5 Hz frequency range compared to control rats (Fig. 6B). Interestingly, significantly (p = 0.038) more spike trains in the non-lesioned hemisphere exhibited ~1 Hz oscillatory activity compared to both control and dopamine lesioned hemispheres (Fig. 6C). There were no significant differences in ISI CV (Fig. 6D), incidence of bursting activity (Fig. 6E) or mean number of bursts per 1000 spikes (Fig. 6F) between the groups.

3.5. Effect of dopamine loss on VAVL LFP activity

LFP activity in VAVL thalamus was also dominated by ~1 Hz oscillatory activity (Fig. 7A). Dopamine cell lesion did not affect total LFP power in the 0.3–2.5 Hz range (Fig. 7B) between control rats (n = 13 rats), non-lesioned (n = 22 rats) and dopamine lesioned (n = 34 rats) hemispheres.

Analysis of ~1 Hz oscillatory waveform shape for VAVL LFPs revealed almost identical differences as MCx LFPs. Specifically, sharpness ratio, but not steepness ratio, was higher in the non-lesioned (p = 0.001; Hedges' g = 1.28) and lesioned (p < 0.0001; Hedges' g = 1.91) hemispheres (Fig. 7C,D). There was a significant cycle-by-cycle positive correlation between steepness ratio and oscillatory amplitude for most LFPs recorded from each hemisphere (p < 0.0001 for all; Fig. 7E). Correlation coefficients for this analysis were, on average, larger in the lesioned (p = 0.003; Hedges' g = 0.48) and non-lesioned (p = 0.005; Hedges' g = 0.43) hemispheres compared to control.

3.6. Cycle-by-cycle oscillatory sharpness asymmetry is correlated between hemispheres and brain regions

Given that we detected increases in oscillatory sharpness asymmetry in LFPs recorded from MCx and VAVL in both lesioned and non-lesioned hemispheres, we wondered whether oscillatory sharpness may covary between brain areas and could potentially index long-range network synchronization. To estimate the degree to which sharpness covaries between ipsilateral MCx and VAVL, and between hemispheres, we performed Spearman's rank correlation of sharpness ratios computed for each cycle from paired LFP recordings (Fig. 8). Correlation coefficients for this analysis were, on average, greater than 0 for each comparison (p < 0.0001). Coefficients were higher for lesioned VAVL-MCx (p < 0.0001; Hedges' g = 1.60) and MCx-MCx (p < 0.0001; Hedges' g = 1.89) pairs compared to VAVL-VAVL pairs (Fig. 8), possibly reflecting the strength of thalamocortical and callosal pathways relative to inter-thalamic connectivity. Importantly, correlation coefficients from VAVL-MCx LFP pairs were significantly greater in dopamine lesioned rats than controls (p = 0.004, Fig. 8; Hedges' g = 0.53). These data indicate that oscillatory sharpness covaries throughout the thalamocortical network, which may provide an additional measure of long-range hyper-synchronization in PD.

3.7. Effect of dopamine loss on LTS bursts in VAVL spiking activity

Although standard measures of single cell VAVL activity were not affected by dopamine cell lesion, it was still possible that LTS burst activity, a distinguishing characteristic of thalamic (output) neurons, might be altered in anesthetized parkinsonian rats. Thalamic neurons

can fire LTS bursts following a period of sustained hyperpolarization (Llinas and Jahnsen, 1982; Deschenes et al., 1984; Jahnsen and Llinas, 1984; Sherman and Guillery, 2006). It is possible that the increased inhibitory bursty and oscillatory activity in basal ganglia output nuclei consistently reported following dopamine depletion (Burbaud et al., 1995; Murer et al., 1997b; Tseng et al., 2001a; Belluscio et al., 2003b; Tseng et al., 2005; Belluscio et al., 2007; Walters et al., 2007) might hyperpolarize VAVL neurons and increase expression of LTS bursts. Therefore, effects of dopamine cell lesion on the incidence and timing of LTS bursts in VAVL were examined.

3.7.1. Incidence of LTS bursts—In the present study, high frequency (>100 Hz) bursts in extracellularly recorded spike trains (Fig. 9A), which met the criteria of LTS bursts established from intracellular recordings (see methods), contained 2–8 spikes. Analysis of VAVL spike trains showed that 22.9% of all ISIs (n = 66,943) from control rats were classified as occurring within LTS bursts. Dopamine cell lesion (17,658/74934, 23.6%) did not alter the proportion of ISIs in LTS bursts compared to control or non-lesioned (16,494/68509, 24.1%) hemispheres. Similarly, the incidence of spike trains that contained at least one LTS burst was not affected by dopamine cell lesion (Fig. 9B); 92.5% (175/189) of VAVL spike trains from control, non-lesioned and lesioned hemispheres exhibited LTS bursts. Most spike trains contained a mixture of LTS bursts (i.e., some combination of doublets, triplets or quadruplets) and dopamine cell lesion didn't alter expression of mixed types of LTS bursts (Fig. 9B). The mean number of LTS bursts per spike train was also not affected by dopaminergic lesion in those spike trains with LTS bursts (Fig. 9B).

The number of spikes in LTS bursts will affect the impact of VAVL activity on downstream structures. Example triplets and quadruplets are shown in Fig. 9A. Dopamine cell lesion did not affect the proportion of LTS bursts classified as doublets, triplets etc. Doublets were the most frequently occurring type of LTS bursts, accounting for 57.3% (11,020/19218) of all LTS bursts across control, non-lesioned and lesioned hemispheres. Triplets and quadruplets were also common, accounting for 29.7% (n = 5700 LTS bursts) and 11.5% (n = 2217) of all LTS bursts, respectively. Few LTS bursts (1.5%, n = 281) contained 5–8 spikes.

3.7.2. ISI of LTS bursts—VAVL LTS burst ISIs in all hemispheres were generally typical of those shown in other thalamic nuclei (Domich et al., 1986; Steriade et al., 1990b). Visual inspection of Fig. 9A shows ISIs were found to be progressively longer within a burst, and the duration of the first ISI is predictive of the total number of spikes in the LTS bursts (Fig. 9C). ISIs were significantly different (p = 0.001) in all comparisons between the first, second, third and fourth ISI in LTS bursts (Fig. 9D). ISIs were also significantly different (p = 0.001) in all comparisons between doublets, triplets, quadruplets and quintuplets (Fig. 9E). Between group analysis showed that dopamine cell lesion was associated with a subtle lengthening of ISIs in LTS bursts, being shortest for the control hemisphere and longest for the dopamine lesioned hemisphere (Fig. 9F). While statistically significant, the detected increase in ISI in dopamine lesioned hemisphere is likely too small (0.4 ms; Hedges' g = 0.53) to reduce temporal summation at downstream targets because the membrane time constant of cortical or striatal neurons following thalamic activation is 5 fold larger (Sugimori et al., 1978; Usrey et al., 2000).

4. Discussion

The present study examined whether MCx and VAVL Mthal neuronal activity are altered in a rat model of PD. Firing rate of layer V, but not layer VI, putative pyramidal neurons in MCx decreased significantly in anesthetized rats 1–2 weeks after 6-OHDA dopaminergic lesion, and was associated with significant loss of dopamine in the striatum and MCx. In contrast, VAVL single unit activity, including LTS bursting, was not affected by 6-OHDA lesion, which is surprising considering that this brain region is a recipient of GABAergic inputs that are overactive in the dopamine-depleted state (Murer et al., 1997a; Lobb and Jaeger, 2015). Although the effects of dopamine cell lesion on single cell activity were dissimilar in MCx and Mthal, LFP changes in both structures were mostly consistent: unilateral dopamine cell lesion bilaterally increased ~1 Hz oscillatory waveform sharpness asymmetry in both structures despite no change in total LFP power.

4.1. Dopamine lesion induced changes in single cell activity

The movement deficits of PD are thought to result from dysfunctional MCx activity (Underwood and Parr-Brownlie, 2021). In the present study, 6-OHDA dopaminergic lesion was associated with a significant decrease in spontaneous firing rate and a significant increase in the frequency of bursts of putative pyramidal neurons in layer V, but not layer VI, in the ipsilesional MCx. Although we did not identify the synaptic targets of putative pyramidal neurons in our recordings, the layer specificity of these changes is consistent with the view that dopaminergic lesion preferentially affects the activity of intra-telencephalic or pyramidal tract neurons located in layer V, but not corticothalamic neurons that are located in layer VI (Shepherd, 2013). These data are consistent with other reports of differentially altered corticostriatal activity in urethane anesthetized 6-OHDA rats (Mallet et al., 2006; Ballion et al., 2008) and indicate that the structure of MCx activity is impaired during the stable brain state of anesthesia. Studies in awake parkinsonian animals, in contrast, have found the resting firing rate of MCx pyramidal neurons to be either unchanged (Doudet et al., 1990; Goldberg et al., 2002; Dejean et al., 2008; Hyland et al., 2019; Rios et al., 2019) or slightly decreased (Parr-Brownlie and Hyland, 2005; Pasquereau and Turner, 2011). Inconsistent findings may reflect the inherently non-stable nature of ‘resting’ cortical activity in the awake state and/or differences in the neuronal population sampled because the excitability of pyramidal tract neurons appears to be selectively reduced in rodents (Chen et al., 2021) and primates (Pasquereau and Turner, 2011). Dysfunctional layer V activity could underlie movement deficits in PD by altering activity in descending motor pathways, an idea that is supported by studies showing that movement-related MCx activity is reduced in parkinsonian animals (Doudet et al., 1990; Watts and Mandir, 1992; Parr-Brownlie and Hyland, 2005; Pasquereau et al., 2016; Hyland et al., 2019) and by stimulation studies (Li et al., 2012; Sanders and Jaeger, 2016; Magno et al., 2019). Changes in bursting characteristics of MCx pyramidal neurons have also been reported; however, effects may be dependent on symptoms, with burstiness decreasing in pyramidal neurons during bradykinetic movements in rats (Parr-Brownlie and Hyland, 2005), whereas burstiness increased during severe akinesia (Goldberg et al., 2002).

We did not detect differences in VAVL firing rate or pattern in dopamine lesioned rats. This result was surprising because previous studies consistently show that antecedent basal ganglia neurons adopt bursty and oscillatory firing patterns after dopamine cell loss in similar anesthetized conditions (Murer et al., 1997a; Belluscio et al., 2003a; Walters et al., 2007; Lobb and Jaeger, 2015). Preserved VAVL firing rate following dopamine lesion might be due to compensatory changes in membrane properties that elevate cell excitability (Bichler et al., 2021), which is in keeping with a recent study that found acute dopaminergic inhibition, but not chronic 6-OHDA lesion, lowered VAVL firing rate (by ~50%) in urethane-anesthetized rats (Di Giovanni et al., 2020). Regardless of the mechanism, our data indicate that VAVL mean discharge rate is unlikely to be an important pathophysiological factor in PD. This view opposes the popular rate model of PD pathophysiology (Albin et al., 1989; DeLong, 1990; Brown and Marsden, 1998; Magnin et al., 2000) but is supported by studies in MPTP-intoxicated primates showing that pallidal DBS generates diverse (predominantly inhibitory) rate changes in Mthal neurons despite improvement in motor function (Anderson et al., 2003; Vitek et al., 2012; Muralidharan et al., 2017).

Preserved VAVL firing pattern following dopamine lesion could be a consequence of how this neuronal population integrates synaptic inputs. Kim et al. (2017) found that VL neurons have complex responses to inhibitory pallidal input, characterized by initial inhibition followed by rebound firing, which could have the effect of smoothing inhibitory input if it arrives in bursts. However, it is also possible that inhibitory bursts arriving from the basal ganglia are counteracted by excitatory bursts of synaptic activity arriving simultaneously from layer V pyramidal neurons (Bosch-Bouju et al., 2013). This hypothesis is supported by our finding that dopamine lesion elevates burst rate in layer V pyramidal neurons and is in keeping with Magnusson and Leventhal's (2021) theory that basal ganglia input modulates the timing of thalamic responses to cortical input.

4.2. LTS burst activity in VAVL thalamus

We found that dopamine lesion did not alter the expression of LTS bursts recorded under anesthesia. This result contrasts previous studies in conscious rats (Bosch-Bouju et al., 2014) and primates (Devergnas et al., 2016) that found dopaminergic lesion increased the occurrence of LTS bursts. However, we found that LTS bursts were more common under urethane-anesthesia (>20/min) compared to that reported in conscious rats (~2/min) (Bosch-Bouju et al., 2014), which is in keeping with other observations that thalamic bursts are more common during periods of inattention (Swadlow and Gusev, 2001; Ramcharan et al., 2005). Thus, by producing a general increase in LTS bursting, anesthesia may have masked differences between control and dopamine cell lesioned rats in the present study.

4.3. Dopamine lesion induced changes in oscillatory LFP activity

Excessive neuronal synchronization is a salient feature of PD. Data from awake Parkinson's patient and animal model field potential recordings consistently report beta (~12–30 Hz) frequency oscillations in basal ganglia and Mthal have greater power and coherence with beta frequencies in MCx (Dejean et al., 2008; Kühn et al., 2009; Avila et al., 2010; Tachibana et al., 2011; Brazhnik et al., 2012; Dejean et al., 2012; Hirschmann et al., 2013; Devergnas et al., 2014; Delaville et al., 2015; Brazhnik et al., 2016; Jávor-Duray et al.,

2017; Cagnan et al., 2019). Evidence also indicates that local beta oscillations in MCx are hyper-synchronized as reflected by increased Fourier power (Sharott et al., 2005; Degos et al., 2009; Brazhnik et al., 2012; Jávor-Duray et al., 2015; Jávor-Duray et al., 2017), changes in temporal dynamics (Yu et al., 2021) or asymmetric waveform shape differences (Cole et al., 2017; Jackson et al., 2019).

In the present study, we examined slow-wave (0.3–2.5 Hz) LFP activity because it dominants the urethane-induced anesthesia brain state where beta oscillations are absent (Contreras and Steriade, 1995; Tseng et al., 2001a; Parr-Brownlie et al., 2007). We found that dopamine lesion influenced the waveform shape, but not total power, of slow-wave LFPs recorded from MCx and VAVL. Specifically, compared to control rats, sharpness asymmetry in dopamine lesioned rats was greater in both hemispheres and more correlated between ipsilateral MCx and VAVL. While we remain cautious in interpreting these data until the neurophysiological basis of sharpness asymmetry is clarified, we predict that sharpness asymmetry correlations between brain structures reflect a spreading of synchrony in light of data showing that sharp troughs in LFP recordings are produced by near-synchronous bursts of excitatory synaptic activity (Sherman et al., 2016). While speculative, this interpretation may also explain why sharpness asymmetry was increased in both hemispheres in unilaterally lesioned rats. Our data support Cole and Voytek's (2017) recommendation that temporal features of oscillatory waveform shape in the time-domain in parkinsonian humans and animal models should complement frequency-domain analyses (Cole and Voytek, 2017).

4.4. Direct and indirect dopaminergic modulation of MCx activity in Parkinson's disease

Detected changes in MCx activity may arise through altered activity in the basal ganglia-thalamocortical pathway or direct loss of dopamine in the MCx. We found that 6-OHDA lesion was associated with substantial (98%) loss of dopamine in the striatum and significant (37%) loss of dopamine in the MCx, consistent with loss of dopamine content or terminals reported in animal models of PD (Pifl et al., 1991; Debeir et al., 2005; Molina-Luna et al., 2009). These data raise the possibility that loss of mesocortical dopamine, which occurs relatively early in PD patients (Gaspar et al., 1991; Moore et al., 2008), directly contributes to dysfunctional pyramidal neuron activity or oscillatory waveform shape differences, especially since we did not detect overt changes in single VAVL cell activity. The influence of mesocortical dopamine on steady-state MCx activity is uncertain, with stimulation studies reporting both excitation and inhibition of pyramidal neurons (Huda et al., 2001; Awenowicz and Porter, 2002; Vitrac et al., 2014).

4.5. Relevance to unanesthetized states

The present investigation examined the functional connectivity of MCx and Mthal in 6-OHDA lesioned rats with electrophysiological recordings obtained under urethane anesthesia. This preparation is informative because it presents a stable brain state that is free of behavioral confounds and dominated by highly-regularized, large amplitude slow oscillations that are generated by the cortex and propagated to the basal ganglia and thalamus (Magill et al., 2001b; Tseng et al., 2001b). Furthermore, the anesthetized state is qualitatively similar to non-rapid eye movement sleep with respect to field potential activity

(Urrestarazu et al., 2009; Thompson et al., 2018) and the occurrence of burst firing in basal ganglia neurons (Urbain et al., 2000; Magill et al., 2001b; Walters et al., 2007). Since sleep is dysfunctional in PD (Garcia-Borreguero et al., 2003), insights gained from anesthetized recordings could highlight putative mechanisms underlying parkinsonian sleep dysfunction.

Nonetheless, data should be interpreted cautiously when considering the functional relevance of results obtained during anesthesia because neurophysiology is perturbed. In that regard, a recent study showed that anesthesia decreases the ability of layer V neurons to fire in response to inputs at their distal apical dendrites (Suzuki and Larkum, 2020), which might explain why, in this study, uniform and cross-correlated changes in waveform shape in thalamic and cortical LFPs were not mirrored by consistent changes in cell activity.

In summary, rats modeling late-stage parkinsonism with 40% loss of dopamine in the MCx exhibited selective hypoactivity and a higher burst rate of layer V, but not layer VI, putative pyramidal neurons. Dopamine-lesion failed to change MCx LFP power, or VAVL Mthal spiking (rate, bursts, oscillations and LTS bursts) and LFP power. In contrast, the sharpness asymmetry of ~1 Hz oscillations increased bilaterally in the MCx and Mthal in parkinsonian rats. Therefore, further studies are warranted to explore if asymmetries in oscillatory sharpness of MCx LFP or EEG, particularly in frequencies present in the awake state (i.e., beta), may be a biometric that can help diagnose or track disease progression in PD patients.

Acknowledgements

The Intramural Research Program of the NINDS, NIH supported this research and the Health Research Council of New Zealand (17-284) for salary support for additional analyses and revisions. We would like to thank Prof. Graeme Eisenhoffer, University of Dresden, for guidance with quantification of dopamine by HPLC.

References

Albin RL, Young AB, Penney JB, 1989. The functional anatomy of basal ganglia disorders. Trends Neurosci 12, 366–375. [PubMed: 2479133]

Aldes LD, 1988. Thalamic connectivity of rat somatic motor cortex. Brain Res. Bull 20, 333–348. [PubMed: 2452673]

Alexander GE, Crutcher MD, 1990. Functional architecture of basal ganglia circuits: neural substrates of parallel processing. Trends Neurosci 13, 266–271. [PubMed: 1695401]

Anderson ME, DeVito JL, 1987. An analysis of potentially converging inputs to the rostral ventral thalamic nuclei of the cat. Exp. Brain Res 68, 260–276. [PubMed: 3691701]

Anderson ME, Turner RS, 1991. Activity of neurons in cerebellar-receiving and pallidal-receiving areas of the thalamus of the behaving monkey. J. Neurophysiol 66, 879–893. [PubMed: 1753292]

Anderson ME, Postupna N, Ruffo M, 2003. Effects of high-frequency stimulation in the internal globus pallidus on the activity of thalamic neurons in the awake monkey. J. Neurophysiol 89, 1150–1160. [PubMed: 12574488]

Avila I, Parr-Brownlie LC, Brazhnik E, Castañeda E, Bergstrom DA, Walters JR, 2010. Beta frequency synchronization in basal ganglia output during rest and walk in a hemiparkinsonian rat. Exp. Neurol 221, 307–319. [PubMed: 19948166]

Awenowicz PW, Porter LL, 2002. Local application of dopamine inhibits pyramidal tract neuron activity in the rodent motor cortex. J. Neurophysiol 88, 3439–3451. [PubMed: 12466459]

Ballion B, Mallet N, Bézard E, Lanciego JL, Gonon F, 2008. Intratelencephalic corticostriatal neurons equally excite striatonigral and striatopallidal neurons and their discharge activity is selectively reduced in experimental parkinsonism. Eur. J. Neurosci 27, 2313–2321. [PubMed: 18445222]

Bartho P, Hirase H, Monconduit L, Zugaro M, Harris KD, Buzsaki G, 2004. Characterization of neocortical principal cells and interneurons by network interactions and extracellular features. J. Neurophysiol 92, 600–608. [PubMed: 15056678]

Bauswein E, Fromm C, Preuss A, 1989. Corticostriatal cells in comparison with pyramidal tract neurons: contrasting properties in the behaving monkey. Brain Res 493, 198–203. [PubMed: 2776007]

Belluscio MA, Kasanetz F, Riquelme LA, Murer MG, 2003a. Spreading of slow cortical rhythms to the basal ganglia output nuclei in rats with nigrostriatal lesions. Eur. J. Neurosci 17, 1046–1052. [PubMed: 12653980]

Belluscio MA, Kasanetz F, Riquelme LA, Murer MG, 2003b. Spreading of slow cortical rhythms to the basal ganglia output nuclei in rats with nigrostriatal lesions. Eur. J. Neurosci 17, 1046–1052. [PubMed: 12653980]

Belluscio MA, Riquelme LA, Murer MG, 2007. Striatal dysfunction increases basal ganglia output during motor cortex activation in parkinsonian rats. Eur. J. Neurosci 25, 2791–2804. [PubMed: 17561844]

Bichler EK, Cavarretta F, Jaeger D, 2021. Changes in excitability properties of ventromedial motor thalamic neurons in 6-OHDA lesioned mice. eNeuro 8.

Boon LI, Geraedts VJ, Hillebrand A, Tannemaat MR, Contarino MF, Stam CJ, Berendse HW, 2019. A systematic review of MEG-based studies in Parkinson's disease: the motor system and beyond. Hum. Brain Mapp 40, 2827–2848. [PubMed: 30843285]

Bosch-Bouju C, Hyland BI, Parr-Brownlie LC, 2013. Motor thalamus integration of cortical, cerebellar and basal ganglia information: implications for normal and parkinsonian conditions. Front. Comput. Neurosci 7, 1–21, 163. [PubMed: 23355821]

Bosch-Bouju C, Smither RA, Hyland BI, Parr-Brownlie LC, 2014. Reduced reach-related modulation of motor thalamus neural activity in a rat model of Parkinson's disease. J. Neurosci 34, 15836–15850. [PubMed: 25429126]

Brazhnik E, Cruz AV, Avila I, Wahba MI, Novikov N, Ilieva NM, McCoy AJ, Gerber C, Walters JR, 2012. State-dependent spike and local field synchronization between motor cortex and substantia nigra in hemiparkinsonian rats. J. Neurosci 32, 7869–7880. [PubMed: 22674263]

Brazhnik E, McCoy AJ, Novikov N, Hatch CE, Walters JR, 2016. Ventral medial thalamic nucleus promotes synchronization of increased high beta oscillatory activity in the basal ganglia-thalamocortical network of the hemiparkinsonian rat. J. Neurosci 36, 4196–4208. [PubMed: 27076419]

Brazhnik E, Novikov N, McCoy AJ, Ilieva NM, Ghraib MW, Walters JR, 2021. Early decreases in cortical mid-gamma peaks coincide with the onset of motor deficits and precede exaggerated beta build-up in rat models for Parkinson's disease. Neurobiol. Dis 155, 105393. [PubMed: 34000417]

Brown P, Marsden CD, 1998. What do the basal ganglia do? Lancet 351, 1801–1804. [PubMed: 9635969]

Burbaud P, Gross C, Benazzouz A, Coussenmacq M, Bioulac B, 1995. Reduction of apomorphine-induced rotational behaviour by subthalamic lesion in 6-OHDA lesioned rats is associated with a normalization of firing rate and discharge pattern of pars reticulata neurons. Exp. Brain Res 105, 48–58. [PubMed: 7589317]

Butler EG, Horne MK, Hawkins NJ, 1992. The activity of monkey thalamic and motor cortical neurones in a skilled, ballistic movement. J. Physiol 445, 25–48. [PubMed: 1501135]

Butler EG, Finkelstein DI, Harvey MC, Churchward PR, Forlano LM, Horne MK, 1996. The relationship between monkey ventrolateral thalamic nucleus activity and kinematic parameters of wrist movement. Brain Res 736, 146–159. [PubMed: 8930319]

Cagnan H, Mallet N, Moll CKE, Gulberti A, Holt AB, Westphal M, Gerloff C, Engel AK, Hamel W, Magill PJ, Brown P, Sharott A, 2019. Temporal evolution of beta bursts in the parkinsonian cortical and basal ganglia network. Proc. Natl. Acad. Sci. U. S. A 116, 16095–16104. [PubMed: 31341079]

Chen L, Daniels S, Kim Y, Chu HY, 2021. Cell type-specific decrease of the intrinsic excitability of motor cortical pyramidal neurons in parkinsonism. J. Neurosci 41, 5553–5565. [PubMed: 34006589]

Cicirata F, Angaut P, Cioni M, Serapide MF, Papale A, 1986. Functional organization of thalamic projections to the motor cortex. An anatomical and electrophysiological study in the rat. Neuroscience 19, 81–99. [PubMed: 3024065]

Cole SR, Voytek B, 2017. Brain oscillations and the importance of waveform shape. Trends Cogn. Sci 21, 137–149. [PubMed: 28063662]

Cole SR, van der Meij R, Peterson EJ, de Hemptinne C, Starr PA, Voytek B, 2017. Nonsinusoidal Beta oscillations reflect cortical pathophysiology in Parkinson's disease. J. Neurosci 37, 4830–4840. [PubMed: 28416595]

Connors BW, Gutnick MJ, 1990. Intrinsic firing patterns of diverse neocortical neurons. Trends Neurosci 13, 99–104. [PubMed: 1691879]

Constantinidis C, Goldman-Rakic PS, 2002. Correlated discharges among putative pyramidal neurons and interneurons in the primate prefrontal cortex. J. Neurophysiol 88, 3487–3497. [PubMed: 12466463]

Contreras D, Steriade M, 1995. Cellular basis of EEG slow rhythms: a study of dynamic corticothalamic relationships. J. Neurosci 15, 604–622. [PubMed: 7823167]

Dacre J, Colligan M, Clarke T, Ammer JJ, Schiemann J, Chamosa-Pino V, Claudi F, Harston JA, Eleftheriou C, Pakan JMP, Huang CC, Hantman AW, Rochefort NL, Duguid I, 2021. A cerebellar-thalamocortical pathway drives behavioral context-dependent movement initiation. Neuron 109, 2326–2338.e2328. [PubMed: 34146469]

de Hemptinne C, Ryapolova-Webb ES, Air EL, Garcia PA, Miller KJ, Ojemann JG, Ostrem JL, Galifianakis NB, Starr PA, 2013. Exaggerated phase-amplitude coupling in the primary motor cortex in Parkinson disease. Proc. Natl. Acad. Sci. U. S. A 110, 4780–4785. [PubMed: 23471992]

Debeir T, Ginestet L, Francois C, Laurens S, Martel JC, Chopin P, Marien M, Colpaert F, Raisman-Vozari R, 2005. Effect of intrastriatal 6-OHDA lesion on dopaminergic innervation of the rat cortex and globus pallidus. Exp. Neurol 193, 444–454. [PubMed: 15869947]

Degos B, Deniau JM, Chavez M, Maurice N, 2009. Chronic but not acute dopaminergic transmission interruption promotes a progressive increase in cortical beta frequency synchronization: relationships to vigilance state and akinesia. Cereb. Cortex 19, 1616–1630. [PubMed: 18996909]

Dejean C, Gross CE, Bioulac B, Boraud T, 2008. Dynamic changes in the cortex-basal ganglia network after dopamine depletion in the rat. J. Neurophysiol 100, 385–396. [PubMed: 18497362]

Dejean C, Nadjar A, Le Moine C, Bioulac B, Gross CE, Boraud T, 2012. Evolution of the dynamic properties of the cortex-basal ganglia network after dopaminergic depletion in rats. Neurobiol. Dis 46, 402–413. [PubMed: 22353564]

Delaville C, McCoy AJ, Gerber CM, Cruz AV, Walters JR, 2015. Subthalamic nucleus activity in the awake hemiparkinsonian rat: relationships with motor and cognitive networks. J. Neurosci 35, 6918–6930. [PubMed: 25926466]

DeLong MR, 1990. Primate models of movement disorders of basal ganglia origin. Trends Neurosci 13, 281–285. [PubMed: 1695404]

DeLong MR, Wichmann T, 2007. Circuits and circuit disorders of the basal ganglia. Arch. Neurol 64, 20–24. [PubMed: 17210805]

Deschenes M, Paradis M, Roy JP, Steriade M, 1984. Electrophysiology of neurons of lateral thalamic nuclei in cat: resting properties and burst discharges. J. Neurophysiol 51, 1196–1219. [PubMed: 6737028]

Devergnas A, Pittard D, Bliwise D, Wichmann T, 2014. Relationship between oscillatory activity in the cortico-basal ganglia network and parkinsonism in MPTP-treated monkeys. Neurobiol. Dis 68, 156–166. [PubMed: 24768805]

Devergnas A, Chen E, Ma Y, Hamada I, Pittard D, Kammermeier S, Mullin AP, Faundez V, Lindsley CW, Jones C, Smith Y, Wichmann T, 2016. Anatomical localization of Cav3.1 calcium channels and electrophysiological effects of T-type calcium channel blockade in the motor thalamus of MPTP-treated monkeys. J. Neurophysiol 115, 470–485. [PubMed: 26538609]

Di Giovanni G, Grandi LC, Fedele E, Orban G, Salvadè A, Song W, Cuboni E, Stefani A, Kaelin-Lang A, Galati S, 2020. Acute and chronic dopaminergic depletion differently affect motor thalamic function. Int. J. Mol. Sci 21, 1–13, 2734.

Domich L, Oakson G, Steriade M, 1986. Thalamic burst patterns in the naturally sleeping cat: a comparison between cortically projecting and reticularis neurones. J. Physiol 379, 429–449. [PubMed: 3560000]

Doudet DJ, Gross C, Arluison M, Bioulac B, 1990. Modifications of precentral cortex discharge and EMG activity in monkeys with MPTP-induced lesions of DA nigral neurons. Exp. Brain Res 80, 177–188. [PubMed: 1972680]

Eisenhofer G, Goldstein DS, Stull R, Keiser HR, Sunderland T, Murphy DL, Kopin IJ, 1986. Simultaneous liquid-chromatographic determination of 3,4-dihydroxyphenylglycol, catecholamines, and 3,4-dihydroxyphenylalanine in plasma, and their responses to inhibition of monoamine oxidase. Clin. Chem 32, 2030–2033. [PubMed: 3096593]

Evarts EV, 1966. Pyramidal tract activity associated with a conditioned hand movement in the monkey. J. Neurophysiol 29, 1011–1027. [PubMed: 4961643]

Forlano LM, Horne MK, Butler EG, Finkelstein D, 1993. Neural activity in the monkey anterior ventrolateral thalamus during trained, ballistic movements. J. Neurophysiol 70, 2276–2288. [PubMed: 8120582]

Gaidica M, Hurst A, Cyr C, Leventhal DK, 2018. Distinct populations of motor thalamic neurons encode action initiation, action selection, and movement vigor. J. Neurosci 38, 6563–6573. [PubMed: 29934350]

Garcia-Borreguero D, Larrosa O, Bravo M, 2003. Parkinson's disease and sleep. Sleep Med. Rev 7, 115–129. [PubMed: 12628213]

Gaspar P, Duyckaerts C, Alvarez C, Javoy-Agid F, Berger B, 1991. Alterations of dopaminergic and noradrenergic innervations in motor cortex in Parkinson's disease. Ann. Neurol 30, 365–374. [PubMed: 1683212]

Gerfen CR, Wilson CJ, 1996. The basal ganglia. In: Swanson LW, Bjorklund A, Hokfelt T (Eds.), Handbook of Chemical Neuroanatomy, vol. 12. Elsevier Science BV, Amsterdam, pp. 371–468.

Goldberg JA, Boraud T, Maraton S, Haber SN, Vaadia E, Bergman H, 2002. Enhanced synchrony among primary motor cortex neurons in the 1-methyl-4-phenyl-1,2,3,6-tetrahydropyridine primate model of Parkinson's disease. J. Neurosci 22, 4639–4653. [PubMed: 12040070]

Gross C, Feger J, Seal J, Haramburu P, Bioulac B, 1983. Neuronal activity in area 4 and movement parameters recorded in trained monkeys after unilateral lesions of the substantia nigra. Exp. Brain. Res. Suppl 7, 181–193.

Guo L, Xiong H, Kim JI, Wu YW, Lalchandani RR, Cui Y, Shu Y, Xu T, Ding JB, 2015. Dynamic rewiring of neural circuits in the motor cortex in mouse models of Parkinson's disease. Nat. Neurosci 18, 1299–1309. [PubMed: 26237365]

Hammond C, Bergman H, Brown P, 2007. Pathological synchronization in Parkinson's disease: networks, models and treatments. Trends Neurosci 30, 357–364. [PubMed: 17532060]

Hazrati LN, Parent A, 1991. Contralateral pallidothalamic and pallidotegmental projections in primates: an anterograde and retrograde labeling study. Brain Res 567, 212–223. [PubMed: 1817727]

Hirschmann J, Özkurt TE, Butz M, Homburger M, Elben S, Hartmann CJ, Vesper J, Wojtecki L, Schnitzler A, 2013. Differential modulation of STN-cortical and cortico-muscular coherence by movement and levodopa in Parkinson's disease. Neuroimage 68, 203–213. [PubMed: 23247184]

Ho J, Tumkaya T, Aryal S, Choi H, Claridge-Chang A, 2019. Moving beyond P values: data analysis with estimation graphics. Nat. Methods 16, 565–566. [PubMed: 31217592]

Horne MK, Porter R, 1980. The discharges during movement of cells in the ventrolateral thalamus of the conscious monkey. J. Physiol 304, 349–372. [PubMed: 7441539]

Huda K, Salunga TL, Matsunami K, 2001. Dopaminergic inhibition of excitatory inputs onto pyramidal tract neurons in cat motor cortex. Neurosci. Lett 307, 175–178. [PubMed: 11438392]

Hyland BI, Seeger-Armbruster S, Smither RA, Parr-Brownlie LC, 2019. Altered recruitment of motor cortex neuronal activity during the grasping phase of skilled reaching in a chronic rat model of unilateral parkinsonism. J. Neurosci 39, 9660–9672. [PubMed: 31641050]

Ilinsky IA, Kultas-Ilinsky K, 2001. Neuroanatomical organization and connections of the motor thalamus in primates. In: Kultas-Ilinsky K, Ilinsky I (Eds.), Basal Ganglia and Thalamus in Health and Movement Disorders Kluwer Academic/Plenum Publishers, New York, pp. 77–91.

Inase M, Buford JA, Anderson ME, 1996. Changes in the control of arm position, movement, and thalamic discharge during local inactivation in the globus pallidus of the monkey. J. Neurophysiol 75, 1087–1104. [PubMed: 8867120]

Ivanusic JJ, Bourke DW, Xu ZM, Butler EG, Horne MK, 2005. Cerebellar thalamic activity in the macaque monkey encodes the duration but not the force or velocity of wrist movement. Brain Res 1041, 181–197. [PubMed: 15829227]

Jackson N, Cole SR, Voytek B, Swann NC, 2019. Characteristics of waveform shape in Parkinson's disease detected with scalp electroencephalography. eNeuro 6.

Jahnsen H, Llinas R, 1984. Electrophysiological properties of guinea-pig thalamic neurones: an in vitro study. J. Physiol 349, 205–226. [PubMed: 6737292]

Jávor-Duray BN, Vinck M, van der Roest M, Mulder AB, Stam CJ, Berendse HW, Voorn P, 2015. Early-onset cortico-cortical synchronization in the hemiparkinsonian rat model. J. Neurophysiol 113, 925–936. [PubMed: 25392174]

Jávor-Duray BN, Vinck M, van der Roest M, Bezard E, Berendse HW, Boraud T, Voorn P, 2017. Alterations in functional cortical hierarchy in Hemiparkinsonian rats. J. Neurosci 37, 7669–7681. [PubMed: 28687605]

Kammermeier S, Pittard D, Hamada I, Wichmann T, 2016. Effects of high-frequency stimulation of the internal pallidal segment on neuronal activity in the thalamus in parkinsonian monkeys. J. Neurophysiol 116, 2869–2881. [PubMed: 27683881]

Kaneoke Y, Vitek JL, 1996. Burst and oscillation as disparate neuronal properties. J. Neurosci. Methods 68, 211–223. [PubMed: 8912194]

Kim J, Kim Y, Nakajima R, Shin A, Jeong M, Park AH, Jeong Y, Jo S, Yang S, Park H, Cho SH, Cho KH, Shim I, Chung JH, Paik SB, Augustine GJ, Kim D, 2017. Inhibitory basal ganglia inputs induce excitatory motor signals in the thalamus. Neuron 95, 1181–1196.e1188. [PubMed: 28858620]

Krack P, Dostrovsky J, Ilinsky I, Kultas-Ilinsky K, Lenz F, Lozano A, Vitek J, 2002. Surgery of the motor thalamus: problems with the present nomenclatures. Mov. Disord 17 (Suppl. 3), S2–S8.

Kühn AA, Tsui A, Aziz T, Ray N, Brücke C, Kupsch A, Schneider GH, Brown P, 2009. Pathological synchronisation in the subthalamic nucleus of patients with Parkinson's disease relates to both bradykinesia and rigidity. Exp. Neurol 215, 380–387. [PubMed: 19070616]

Kunimatsu J, Tanaka M, 2010. Roles of the primate motor thalamus in the generation of antisaccades. J. Neurosci 30, 5108–5117. [PubMed: 20371831]

Kuramoto E, Fujiyama F, Nakamura KC, Tanaka Y, Hioki H, Kaneko T, 2011. Complementary distribution of glutamatergic cerebellar and GABAergic basal ganglia afferents to the rat motor thalamic nuclei. Eur. J. Neurosci 33, 95–109. [PubMed: 21073550]

Kurata K, 2005. Activity properties and location of neurons in the motor thalamus that project to the cortical motor areas in monkeys. J. Neurophysiol 94, 550–566. [PubMed: 15703228]

Lacey CJ, Bolam JP, Magill PJ, 2007. Novel and distinct operational principles of intralaminar thalamic neurons and their striatal projections. J. Neurosci 27, 4374–4384. [PubMed: 17442822]

Larkum ME, Senn W, Lüscher HR, 2004. Top-down dendritic input increases the gain of layer 5 pyramidal neurons. Cereb. Cortex 14, 1059–1070. [PubMed: 15115747]

Levy S, Lavzin M, Benisty H, Ghanayim A, Dubin U, Achvat S, Brosh Z, Aeed F, Mensh BD, Schiller Y, Meir R, Barak O, Talmon R, Hantman AW, Schiller J, 2020. Cell-type-specific outcome representation in the primary motor cortex. Neuron 107 (5), 954–971. [PubMed: 32589878]

Li Q, Ke Y, Chan DC, Qian ZM, Yung KK, Ko H, Arbuthnott GW, Yung WH, 2012. Therapeutic deep brain stimulation in parkinsonian rats directly influences motor cortex. Neuron 76, 1030–1041. [PubMed: 23217750]

Lindvall O, Bjorklund A, 1974. The organization of the ascending catecholamine neuron systems in the rat brain. Acta Physiol. Scand Suppl. 412, 1–48.

Llinas R, Jahnsen H, 1982. Electrophysiology of mammalian thalamic neurones in vitro. Nature 297, 406–408. [PubMed: 7078650]

Lobb CJ, Jaeger D, 2015. Bursting activity of substantia nigra pars reticulata neurons in mouse parkinsonism in awake and anesthetized states. Neurobiol. Dis 75, 177–185. [PubMed: 25576395]

Macpherson JM, Rasmusson DD, Murphy JT, 1980. Activities of neurons in “motor” thalamus during control of limb movement in the primate. J. Neurophysiol 44, 11–28. [PubMed: 7420130]

Magill PJ, Bolam JP, Bevan MD, 2001a. Dopamine regulates the impact of the cerebral cortex on the subthalamic nucleus-globus pallidus network. Neuroscience 106, 313–330. [PubMed: 11566503]

Magill PJ, Bolam JP, Bevan MD, 2001b. Dopamine regulates the impact of the cerebral cortex on the subthalamic nucleus-globus pallidus network. Neuroscience 106, 313–330. [PubMed: 11566503]

Magnin M, Morel A, Jeanmonod D, 2000. Single-unit analysis of the pallidum, thalamus and subthalamic nucleus in parkinsonian patients. Neuroscience 96, 549–564. [PubMed: 10717435]

Magno LAV, Tenza-Ferrer H, Collodetti M, Aguiar MFG, Rodrigues APC, da Silva RS, Silva JDP, Nicolau NF, Rosa DVF, Birbrair A, Miranda DM, Romano-Silva MA, 2019. Optogenetic stimulation of the M2 cortex reverts motor dysfunction in a mouse model of Parkinson’s disease. J. Neurosci 39, 3234–3248. [PubMed: 30782975]

Magnusson JL, Leventhal DK, 2021. Revisiting the “paradox of stereotaxic surgery”: insights into basal ganglia-thalamic interactions. Front. Syst. Neurosci 15, 725876. [PubMed: 34512279]

Mallet N, Ballion B, Le Moine C, Gonon F, 2006. Cortical inputs and GABA interneurons imbalance projection neurons in the striatum of parkinsonian rats. J. Neurosci 26, 3875–3884. [PubMed: 16597742]

McFarland NR, Haber SN, 2002. Thalamic relay nuclei of the basal ganglia form both reciprocal and nonreciprocal connections, linking multiple frontal cortical areas. J. Neurosci 22, 8117–8132. [PubMed: 12223566]

Molina-Luna K, Pekanovic A, Rohrich S, Hertler B, Schubring-Giese M, Rioult-Pedotti MS, Luft AR, 2009. Dopamine in motor cortex is necessary for skill learning and synaptic plasticity. PLoS One 4, e7082. [PubMed: 19759902]

Moore RY, Whone AL, Brooks DJ, 2008. Extrastriatal monoamine neuron function in Parkinson’s disease: an 18F-dopa PET study. Neurobiol. Dis 29, 381–390. [PubMed: 18226536]

Muralidharan A, Zhang J, Ghosh D, Johnson MD, Baker KB, Vitek JL, 2017. Modulation of neuronal activity in the motor thalamus during GPi-DBS in the MPTP nonhuman primate model of Parkinson’s disease. Brain Stimul 10, 126–138. [PubMed: 27839724]

Murer MG, Riquelme LA, Tseng KY, Pazo JH, 1997a. Substantia nigra pars reticulata single unit activity in normal and 60HDA-lesioned rats: effects of intrastriatal apomorphine and subthalamic lesions. Synapse 27, 278–293. [PubMed: 9372551]

Murer MG, Riquelme LA, Tseng KY, Pazo JH, 1997b. Substantia nigra pars reticulata single unit activity in normal and 6-OHDA-lesioned rats: effects of intrastriatal apomorphine and subthalamic lesions. Synapse 27, 278–293. [PubMed: 9372551]

Nakamura KC, Sharott A, Magill PJ, 2014. Temporal coupling with cortex distinguishes spontaneous neuronal activities in identified basal ganglia-recipient and cerebellar-recipient zones of the motor thalamus. Cereb. Cortex 24, 81–97. [PubMed: 23042738]

Nambu A, Yoshida S, Jinnai K, 1991. Movement-related activity of thalamic neurons with input from the globus pallidus and projection to the motor cortex in the monkey. Exp. Brain Res 84, 279–284. [PubMed: 2065734]

O’Keeffe AB, Malekmohammadi M, Sparks H, Pouratian N, 2020. Synchrony drives motor cortex Beta bursting, waveform dynamics, and phase-amplitude coupling in Parkinson’s disease. J. Neurosci 40, 5833–5846. [PubMed: 32576623]

Olsson M, Nikkhah G, Bentlage C, Bjorklund A, 1995. Forelimb akinesia in the rat Parkinson model: differential effects of dopamine agonists and nigral transplants as assessed by a new stepping test. J. Neurosci 15, 3863–3875. [PubMed: 7751951]

Paŕe D, Steriade M, Deschênes M, Oakson G, 1987. Physiological characteristics of anterior thalamic nuclei, a group devoid of inputs from reticular thalamic nucleus. J. Neurophysiol 57, 1669–1685. [PubMed: 3037038]

Park J, Coddington LT, Dudman JT, 2020. Basal ganglia circuits for action specification. Annu. Rev. Neurosci 43, 485–507. [PubMed: 32303147]

Parr-Brownlie LC, Hyland BI, 2005. Bradykinesia induced by dopamine D2 receptor blockade is associated with reduced motor cortex activity in the rat. J. Neurosci 25, 5700–5709. [PubMed: 15958736]

Parr-Brownlie LC, Poloskey SL, Flanagan KK, Eisenhofer G, Bergstrom DA, Walters JR, 2007. Dopamine lesion-induced changes in subthalamic nucleus activity are not associated with alterations in firing rate or pattern in layer V neurons of the anterior cingulate cortex in anesthetized rats. Eur. J. Neurosci 26, 1925–1939. [PubMed: 17897398]

Parr-Brownlie LC, Poloskey SL, Bergstrom DA, Walters JR, 2009. Parafascicular thalamic nucleus activity in a rat model of Parkinson's disease. Exp. Neurol 217, 269–281. [PubMed: 19268664]

Pasquereau B, Turner RS, 2011. Primary motor cortex of the parkinsonian monkey: differential effects on the spontaneous activity of pyramidal tract-type neurons. Cereb. Cortex 21, 1362–1378. [PubMed: 21045003]

Pasquereau B, DeLong MR, Turner RS, 2016. Primary motor cortex of the parkinsonian monkey: altered encoding of active movement. Brain 139, 127–143. [PubMed: 26490335]

Paxinos G, Watson C, 1997. The Rat Brain in Stereotaxic Coordinates Academic Press Inc., San Diego.

Percheron G, Talbi CFB, Yelnik J, Fénelon G, 1996. The primate motor thalamus. Brain Res. Rev 22, 93–181. [PubMed: 8883918]

Pessiglione M, Guehl D, Rolland AS, Francois C, Hirsch EC, Feger J, Tremblay L, 2005. Thalamic neuronal activity in dopamine-depleted primates: evidence for a loss of functional segregation within basal ganglia circuits. J. Neurosci 25, 1523–1531. [PubMed: 15703406]

Pifl C, Schingnitz G, Hornykiewicz O, 1991. Effect of 1-methyl-4-phenyl-1,2,3,6-tetrahydropyridine on the regional distribution of brain monoamines in the rhesus monkey. Neuroscience 44, 591–605. [PubMed: 1754053]

Raeva S, Vainberg N, Tikhonov Y, Tsetlin I, 1999. Analysis of evoked activity patterns of human thalamic ventrolateral neurons during verbally ordered voluntary movements. Neuroscience 88, 377–392. [PubMed: 10197761]

Rajakumar N, Elisevich K, Flumerfelt BA, 1994. Parvalbumin-containing GABAergic neurons in the basal ganglia output system of the rat. J. Comp. Neurol 350, 324–336. [PubMed: 7884046]

Ramcharan EJ, Gnadt JW, Sherman SM, 2005. Higher-order thalamic relays burst more than first-order relays. Proc. Natl. Acad. Sci. U. S. A 102, 12236–12241. [PubMed: 16099832]

Rao SG, Williams GV, Goldman-Rakic PS, 1999. Isodirectional tuning of adjacent interneurons and pyramidal cells during working memory: evidence for microcolumnar organization in PFC. J. Neurophysiol 81, 1903–1916. [PubMed: 10200225]

Rios A, Soma S, Yoshida J, Nonomura S, Kawabata M, Sakai Y, Isomura Y, 2019. Differential changes in the lateralized activity of identified projection neurons of motor cortex in Hemiparkinsonian rats. eNeuro 6, 1–19. ENEURO.0110-0119.2019.

Rouiller EM, Moret V, Liang F, 1993. Comparison of the connectional properties of the two forelimb areas of the rat sensorimotor cortex: support for the presence of a premotor or supplementary motor cortical area. Somatosens. Mot. Res 10, 269–289. [PubMed: 8237215]

Saiki A, Sakai Y, Fukabori R, Soma S, Yoshida J, Kawabata M, Yawo H, Kobayashi K, Kimura M, Isomura Y, 2018. In vivo spiking dynamics of intra- and Extratelencephalic projection neurons in rat motor cortex. Cereb. Cortex 28, 1024–1038. [PubMed: 28137723]

Sakai ST, Inase M, Tanji J, 1996. Comparison of cerebellothalamic and pallidothalamic projections in the monkey (Macaca fuscata): a double anterograde labeling study. J. Comp. Neurol 368, 215–228. [PubMed: 8725303]

Sakai ST, Stepniewska I, Qi HX, Kaas JH, 2000. Pallidal and cerebellar afferents to pre-supplementary motor area thalamocortical neurons in the owl monkey: a multiple labeling study. J. Comp. Neurol 417, 164–180. [PubMed: 10660895]

Sanders TH, Jaeger D, 2016. Optogenetic stimulation of cortico-subthalamic projections is sufficient to ameliorate bradykinesia in 6-ohda lesioned mice. Neurobiol. Dis 95, 225–237. [PubMed: 27452483]

Sauerbrei BA, Guo JZ, Cohen JD, Mischiati M, Guo W, Kabra M, Verma N, Mensh B, Branson K, Hantman AW, 2020. Cortical pattern generation during dexterous movement is input-driven. Nature 577, 386–391. [PubMed: 31875851]

Schlag-Rey M, Schlag J, 1984. Visuomotor functions of central thalamus in monkey. I. Unit activity related to spontaneous eye movements. J. Neurophysiol 51, 1149–1174. [PubMed: 6737026]

Schmied A, Bénita M, Condé H, Dormont JF, 1979. Activity of ventrolateral thalamic neurons in relation to a simple reaction time task in the cat. Exp. Brain Res 36, 285–300. [PubMed: 488203]

Schneider JS, Rothblat DS, 1996. Alterations in intralaminar and motor thalamic physiology following nigrostriatal dopamine depletion. Brain Res 742, 25–33. [PubMed: 9117401]

Sharott A, Magill PJ, Harnack D, Kupsch A, Meissner W, Brown P, 2005. Dopamine depletion increases the power and coherence of beta-oscillations in the cerebral cortex and subthalamic nucleus of the awake rat. Eur. J. Neurosci 21, 1413–1422. [PubMed: 15813951]

Shepherd GM, 2013. Corticostriatal connectivity and its role in disease. Nat. Rev. Neurosci 14, 278–291. [PubMed: 23511908]

Sherman SM, Guillery RW, 2006. Exploring the Thalamus and its Role in Cortical Function, (2nd Ed) edition. The MIT Press, Cambridge, MA.

Sherman MA, Lee S, Law R, Haegens S, Thorn CA, Hämäläinen MS, Moore CI, Jones SR, 2016. Neural mechanisms of transient neocortical beta rhythms: converging evidence from humans, computational modeling, monkeys, and mice. Proc. Natl. Acad. Sci. U. S. A 113, E4885–E4894. [PubMed: 27469163]

Shirahige L, Berenguer-Rocha M, Mendonça S, Rocha S, Rodrigues MC, Monte-Silva K, 2020. Quantitative electroencephalography characteristics for Parkinson's disease: a systematic review. J. Parkinsons Dis 10, 455–470. [PubMed: 32065804]

Shrager RI, 2003. On a three-term variant of the Lomb periodogram. Astrophys. Space Sci 277, 519–530.

Sommer MA, 2003. The role of the thalamus in motor control. Curr. Opin. Neurobiol 13, 663–670. [PubMed: 14662366]

Steriade M, Deschenes M, Domich L, Mulle C, 1985. Abolition of spindle oscillations in thalamic neurons disconnected from nucleus reticularis thalami. J. Neurophysiol 54, 1473–1497. [PubMed: 4087044]

Steriade M, Jones EG, Llinas RR, 1990a. Intrinsic properties and ionic conductances of thalamic cells. In: Thalamic Oscillations and Signaling Neurosciences Research Foundation Inc., New York, pp. 115–138.

Steriade M, Jones EG, Llinas RR, 1990b. The oscillatory mode during EEG-synchronized sleep. In: Thalamic Oscillations and Signaling Neurosciences Research Foundation Inc., New York, pp. 167–237.

Strick PL, 1976. Activity of ventrolateral thalamic neurons during arm movement. J. Neurophysiol 39, 1032–1044. [PubMed: 824408]

Sugimori M, Preston RJ, Kitai ST, 1978. Response properties and electrical constants of caudate nucleus neurons in the cat. J. Neurophysiol 41, 1662–1675. [PubMed: 731295]

Suzuki M, Larkum ME, 2020. General anesthesia decouples cortical pyramidal neurons. Cell 180, 666–676.e613. [PubMed: 32084339]

Swadlow HA, Gusev AG, 2001. The impact of 'bursting' thalamic impulses at a neocortical synapse. Nat. Neurosci 4, 402–408. [PubMed: 11276231]

Tachibana Y, Iwamuro H, Kita H, Takada M, Nambu A, 2011. Subthalamo-pallidal interactions underlying parkinsonian neuronal oscillations in the primate basal ganglia. Eur. J. Neurosci 34, 1470–1484. [PubMed: 22034978]

Takahashi N, Moberg S, Zolnik TA, Catanese J, Sachdev RNS, Larkum ME, Jaeger D, 2021. Thalamic input to motor cortex facilitates goal-directed action initiation. Curr. Biol 31, 4148–4155.e4144. [PubMed: 34302741]

Tanaka YH, Tanaka YR, Kondo M, Terada SI, Kawaguchi Y, Matsuzaki M, 2018. Thalamocortical axonal activity in motor cortex exhibits layer-specific dynamics during motor learning. Neuron 100, 244–258.e212. [PubMed: 30174116]

Tassin JP, Bockaert J, Blanc G, Stinus L, Thierry AM, Lavielle S, Premont J, Glowinski J, 1978. Topographical distribution of dopaminergic innervation and dopaminergic receptors of the anterior cerebral cortex of the rat. Brain Res 154, 241–251. [PubMed: 687994]

Thompson JA, Tekriwal A, Felsen G, Ozturk M, Telkes I, Wu J, Ince NF, Abosch A, 2018. Sleep patterns in Parkinson's disease: direct recordings from the subthalamic nucleus. J. Neurol. Neurosurg. Psychiatry 89, 95–104. [PubMed: 28866626]

Thura D, Cisek P, 2017. The basal ganglia do not select reach targets but control the urgency of commitment. Neuron 95, 1160–1170.e1165. [PubMed: 28823728]

Tierney PL, Degenetais E, Thierry AM, Glowinski J, Gioanni Y, 2004. Influence of the hippocampus on interneurons of the rat prefrontal cortex. Eur. J. Neurosci 20, 514–524. [PubMed: 15233760]

Tseng KY, Kasanetz F, Kargieman L, Riquelme LA, Murer MG, 2001a. Cortical slow oscillatory activity is reflected in the membrane potential and spike trains of striatal neurons in rats with chronic nigrostriatal lesions. J. Neurosci 21, 6430–6439. [PubMed: 11487667]

Tseng KY, Kasanetz F, Kargieman L, Pazo JH, Murer MG, Riquelme LA, 2001b. Subthalamic nucleus lesions reduce low frequency oscillatory firing of substantia nigra pars reticulata neurons in a rat model of Parkinson's disease. Brain Res 904, 93–103. [PubMed: 11516415]

Tseng KY, Kargieman L, Gacio S, Riquelme LA, Murer MG, 2005. Consequences of partial and severe dopaminergic lesion on basal ganglia oscillatory activity and akinesia. Eur. J. Neurosci 22, 2579–2586. [PubMed: 16307600]

Tseng KY, Mallet N, Toreson KL, Le Moine C, Gonon F, O'Donnell P, 2006. Excitatory response of prefrontal cortical fast-spiking interneurons to ventral tegmental area stimulation in vivo. Synapse 59, 412–417. [PubMed: 16485264]

Turner RS, DeLong MR, 2000. Corticostriatal activity in primary motor cortex of the macaque. J. Neurosci 20, 7096–7108. [PubMed: 10995857]

Underwood CF, Parr-Brownlie LC, 2021. Primary motor cortex in Parkinson's disease: functional changes and opportunities for neurostimulation. Neurobiol. Dis 147, 105159. [PubMed: 33152506]

Urbain N, Gervasoni D, Soulìere F, Lobo L, Rentéro N, Windels F, Astier B, Savasta M, Fort P, Renaud B, Luppi PH, Chouvet G, 2000. Unrelated course of subthalamic nucleus and globus pallidus neuronal activities across vigilance states in the rat. Eur. J. Neurosci 12, 3361–3374. [PubMed: 10998119]

Urrestarazu E, Iriarte J, Alegre M, Clavero P, Rodríguez-Oroz MC, Guridi J, Obeso JA, Artieda J, 2009. Beta activity in the subthalamic nucleus during sleep in patients with Parkinson's disease. Mov. Disord 24, 254–260. [PubMed: 18951542]

Usrey WM, Alonso JM, Reid RC, 2000. Synaptic interactions between thalamic inputs to simple cells in cat visual cortex. J. Neurosci 20, 5461–5467. [PubMed: 10884329]

Vila M, Périer C, Féger J, Yelnik J, Faucheux B, Ruberg M, Raisman-Vozari R, Agid Y, Hirsch EC, 2000. Evolution of changes in neuronal activity in the subthalamic nucleus of rats with unilateral lesion of the substantia nigra assessed by metabolic and electrophysiological measurements. Eur. J. Neurosci 12, 337–344. [PubMed: 10651888]

Vitek JL, Zhang J, Hashimoto T, Russo GS, Baker KB, 2012. External pallidal stimulation improves parkinsonian motor signs and modulates neuronal activity throughout the basal ganglia thalamic network. Exp. Neurol 233, 581–586. [PubMed: 22001773]

Vitrac C, Péron S, Frappé I, Fernagut PO, Jaber M, Gaillard A, Benoit-Marand M, 2014. Dopamine control of pyramidal neuron activity in the primary motor cortex via D2 receptors. Front Neural Circuits 8, 1–8, 13. [PubMed: 24478635]

Voloshin MY, Lukhanina EP, Kolomietz BP, Prokopenko VF, Rodionov VA, 1994. Electrophysiological investigation of thalamic neuronal mechanisms of motor disorders in parkinsonism: an influence of D2ergic transmission blockade on excitation and inhibition of relay neurons in motor thalamic nuclei of cat. Neuroscience 62, 771–781. [PubMed: 7870305]

Walters JR, Hu D, Itoga CA, Parr-Brownlie LC, Bergstrom DA, 2007. Phase relationships support a role for coordinated activity in the indirect pathway in organizing slow oscillations in basal ganglia output after loss of dopamine. Neuroscience 144, 762–776. [PubMed: 17112675]

Wang Y, Kurata K, 1998. Quantitative analyses of thalamic and cortical origins of neurons projecting to the rostral and caudal forelimb motor areas in the cerebral cortex of rats. Brain Res 781, 137–147. [PubMed: 9507093]

Watts RL, Mandir AS, 1992. The role of motor cortex in the pathophysiology of voluntary movement deficits associated with parkinsonism. Neurol. Clin 10, 451–469. [PubMed: 1584184]

Whishaw IQ, Pellis SM, Gorny BP, 1992. Skilled reaching in rats and humans: evidence for parallel development or homology. Behav. Brain Res 47, 59–70. [PubMed: 1571101]

Wilson FA, O'Scalaidhe SP, Goldman-Rakic PS, 1994. Functional synergism between putative gamma-aminobutyrate-containing neurons and pyramidal neurons in prefrontal cortex. PNAS 91, 4009–4013. [PubMed: 8171027]

Winfield DA, Gatter KC, Powell TP, 1980. An electron microscopic study of the types and proportions of neurons in the cortex of the motor and visual areas of the cat and rat. Brain 103, 245–258. [PubMed: 6772267]

Yu Y, Escobar Sanabria D, Wang J, Hendrix CM, Zhang J, Nebeck SD, Amundson AM, Busby ZB, Bauer DL, Johnson MD, Johnson LA, Vitek JL, 2021. Parkinsonism alters Beta burst dynamics across the basal ganglia-motor cortical network. J. Neurosci 41, 2274–2286. [PubMed: 33483430]

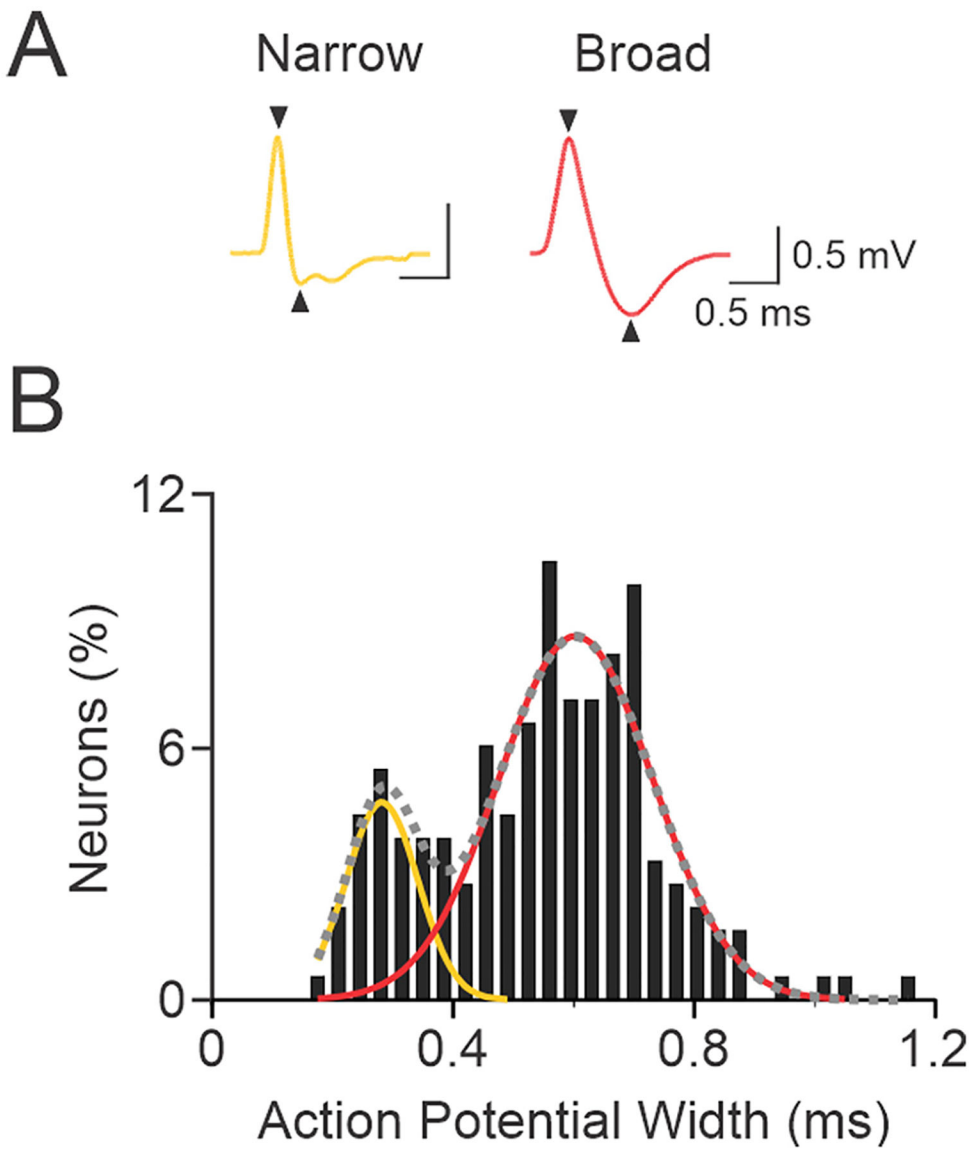

Fig. 1.

Bimodal distribution of action potential width. **A**, Panel shows the extracellular action potential from two neurons recorded in the motor cortex. For these waveforms, action potential width was measured from the peak in the positive deflection to the trough in the negative deflection as indicated by the arrowheads on the waveforms. Action potential widths are 0.228 ms and 0.631 ms for the left and right waveforms, respectively. **B**, Panel shows a normalized distribution of action potential width for neurons (n = 183) recorded in the motor cortex. The dashed gray line shows the weighted sum of two Gaussian curves fitted to the population data (r^2 = 0.84). The mean ± SD of the two peaks from the bimodal distribution were 0.282 ± 0.060 ms and 0.603 ± 0.128 ms. The left and right Gaussian curves (yellow and red lines) show the distribution for narrow and broad waveforms, respectively. Statistically, some neurons (n = 10, 5.5%) had waveforms that were within the mean ± 2 SD of both narrow and broad waveform groups, and these neurons were classified as an

intermediate group (unfilled bars). Action potential waveform widths that were ≥ 0.400 ms were classified as broad (putative pyramidal neurons), waveform widths ≤0.347 ms were classified as narrow (putative interneurons), and waveforms between 0.348 and 0.399 ms were classified in the intermediate group.

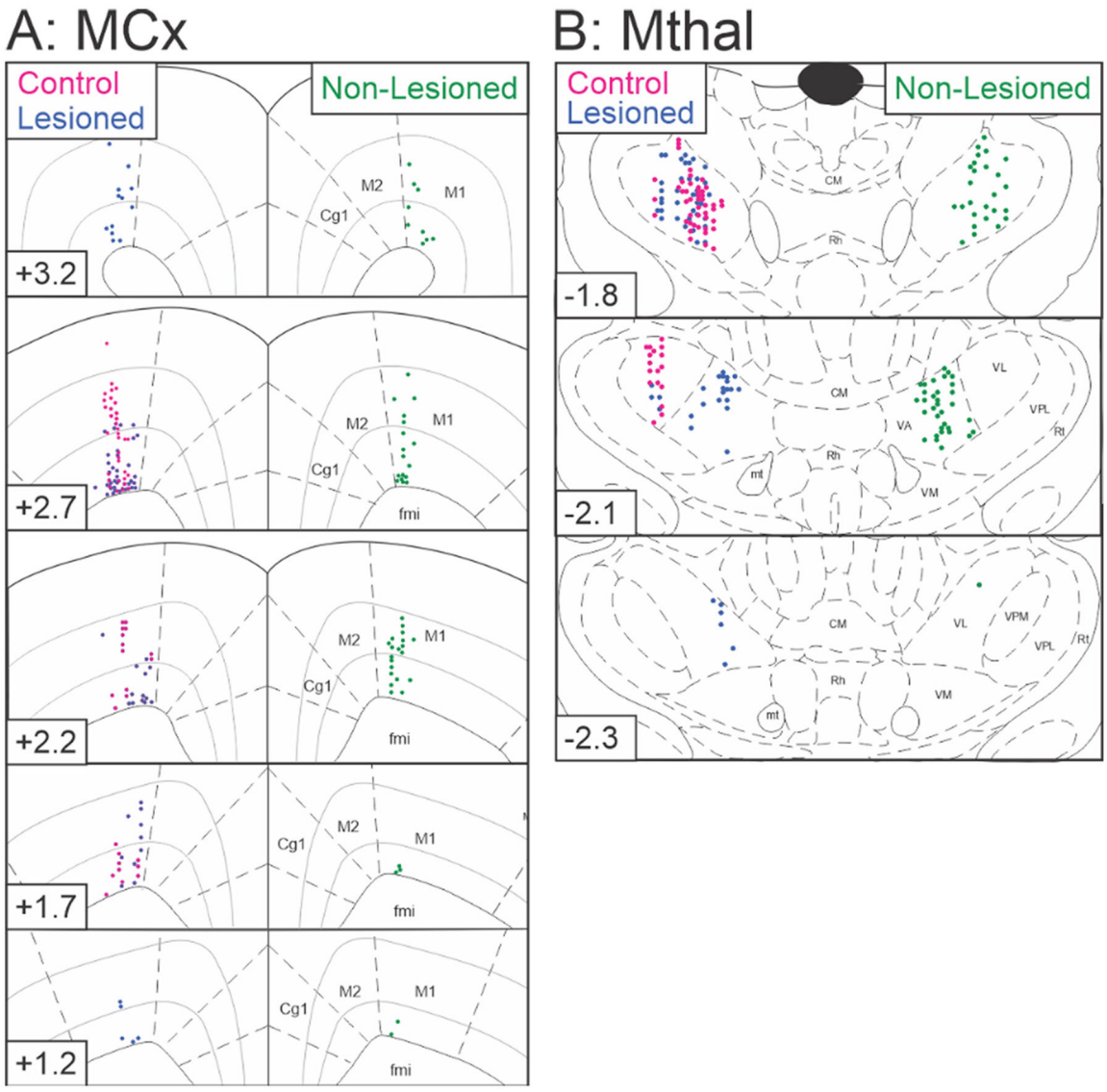

Fig. 2.

A schematic diagram of recording sites in MCx and VAVL thalamus. **A**, MCx recording sites in control rats (n = 57, red) and dopamine lesioned (n = 75, blue) and non-lesioned (n = 51, green) hemispheres reconstructed in the coronal plane on standard atlas sections (Paxinos and Watson, 1997). Note, the neuron recorded in layer II/III in the control hemisphere was included in the analysis to determine putative neuronal type (see Fig. 1 above), but was not included in any other analyses. **B**, VAVL Mthal recording sites in control rats (n = 63, red) and dopamine lesioned (n = 66, blue) and non-lesioned (n = 60, green) hemispheres. Distance (mm) relative to bregma is indicated in the lower left portion of each coronal section. Abbreviations: Cg1 anterior cingulate cortex, CM central median thalamic nucleus, fmi forceps minor corpus callosum, M1 primary motor cortex, M2 secondary motor cortex, mt mammillothalamic tract, Rh rhomboid thalamic nucleus, Rt reticular thalamic nucleus, VA ventroanterior thalamic nucleus, VL ventrolateral thalamic

nucleus, VM ventromedial thalamic nucleus, VPL ventroposterior lateral thalamic nucleus, VPM ventroposterior medial thalamic nucleus.

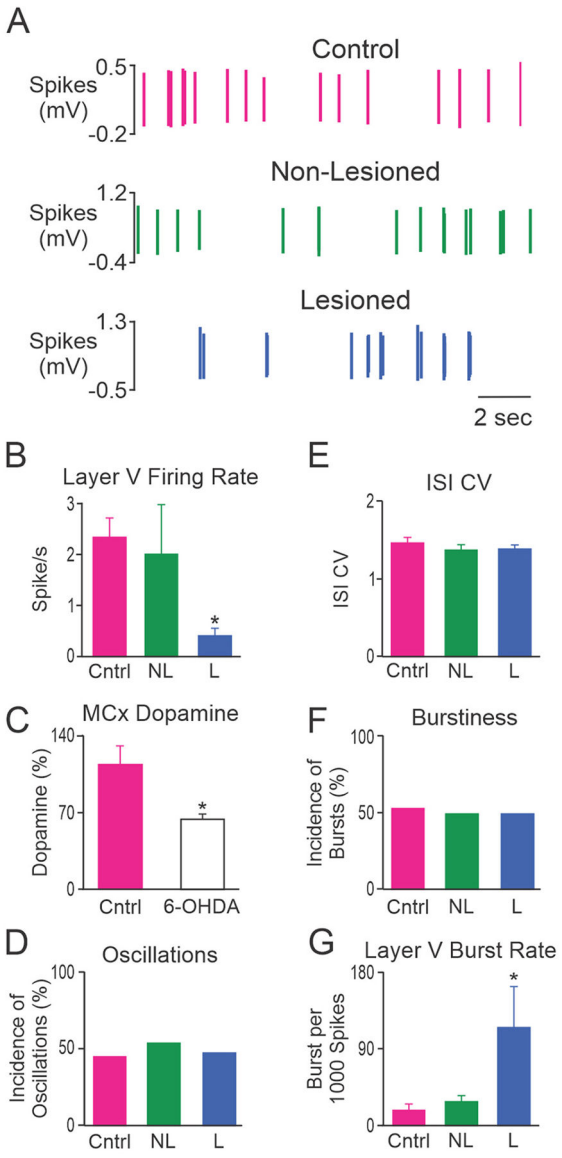

Fig. 3.

Characteristics of MCx spike trains from putative pyramidal neurons. **A**, Representative example of putative pyramidal neuron spike trains from control rats (Cntrl; top, red), and non-lesioned (NL; middle, green) and dopamine lesioned (L; bottom, blue) hemispheres of unilateral 6-OHDA lesioned rats. These 3 neurons were recorded in layer V and had firing rates of 2.84 spikes/s, 2.77 spikes/s and 0.19 spikes/s, respectively. Grouped data showing: **B**, the mean firing rate of putative pyramidal neurons in layer V; **C**, MCx dopamine content detected with HPLC and expressed as a percentage of the non-lesioned hemisphere; **D**, incidence of spike trains with significant 0.3–2.5 Hz oscillatory activity; **E**, mean ISI CV; **F**, incidence of bursty spike trains; and **G**, burst rate for putative pyramidal neurons in layer V. Layer V putative pyramidal neurons fired less frequently and with more bursts in the lesioned hemisphere relative to control rats. * Significant difference of $p < 0.05$ compared to control rats. Total cells: $n = 56$ from 9 Cntrl rats, $n = 51$ from 26 NL hemispheres and

n = 75 from 30 L hemispheres. Layer V cells: *n* = 18 from 6 Cntrl rats, *n* = 17 from 9 NL hemispheres and *n* = 13 from 8 L hemispheres.

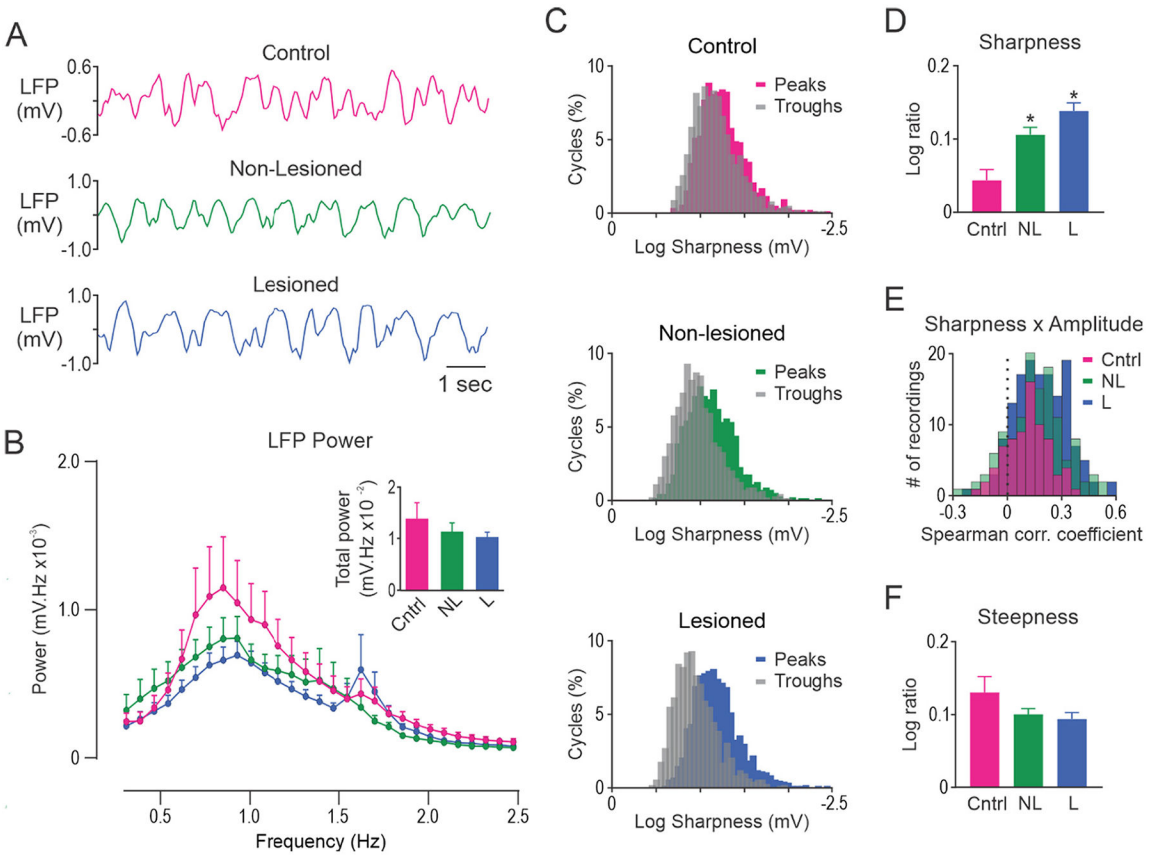

Fig. 4.

Unilateral dopamine lesion alters the shape of slow-wave oscillations in MCx but does not alter FFT power. **A**, Representative segments of MCx LFP activity in control rats (Cntrl; top, red), and non-lesioned (NL; middle, green) and dopamine lesioned (L; bottom, blue) hemispheres of unilateral 6-OHDA lesioned rats. **B**, FFT power spectral density over the 0.3–2.5 Hz range. Total power was not different between the groups (inset). **C**, Histograms showing the distribution of slow-wave peak and trough sharpness in a representative 300 s LFP recording in control rats (top), and non-lesioned (middle) and lesioned (bottom) hemispheres in unilateral 6-OHDA lesioned rats. **D**, Sharpness ratio was significantly larger in non-lesioned and lesioned hemispheres relative to control rats. **E**, On average, a positive correlation between cycle sharpness ratio and amplitude was observed for LFPs recorded from control rats and both hemispheres in 6-OHDA lesioned rats. **F**, Steepness ratio did not differ between control rats, non-lesioned and lesioned hemispheres. * Significant difference of $p < 0.05$ compared to control rats. LFP's recorded from different electrode tracks were averaged to give a single data point for each rat. $n = 14$ Cntrl, $n = 31$ NL and $n = 43$ L.

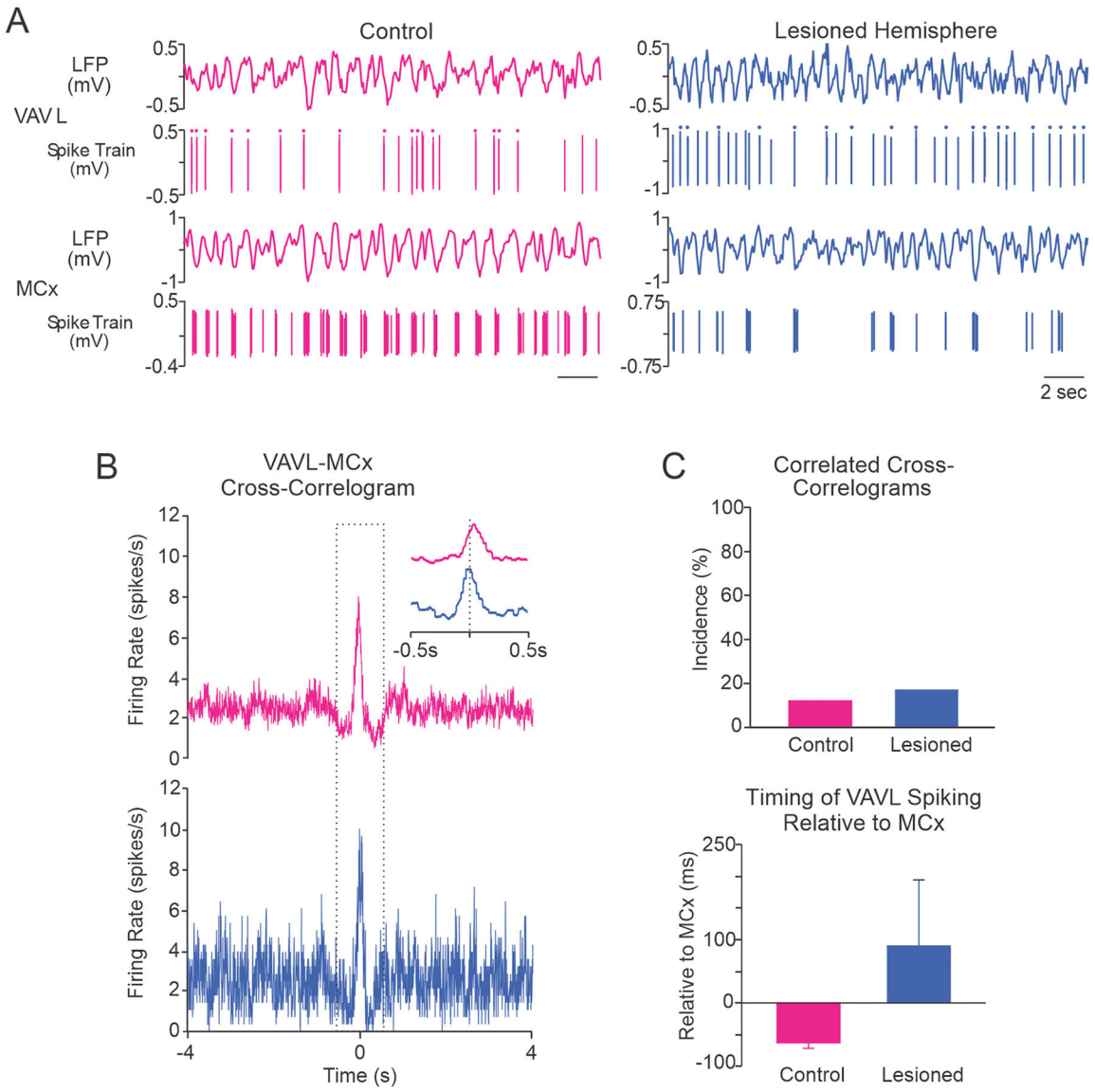

Fig. 5.

Correlated activity between VAVL neurons and putative pyramidal neurons in MCx. **A**, Representative examples of simultaneously recorded spike trains and LFPs from VAVL and putative pyramidal neurons in MCx show coincident oscillations in spiking activity in the control (red) and dopamine lesioned hemisphere (blue). The dots above spikes in spike trains indicate LTS bursts. **B**, MCx-triggered VAVL cross-correlograms from representative spike trains from control and dopamine lesioned hemispheres shown in A above. Cross-correlogram in the control hemisphere (top) shows that neuronal spiking was significantly correlated between VAVL and MCx. The peak in VAVL spiking occurred 46 ms before MCx spikes. For the lesioned hemisphere (bottom), the peak in VAVL spiking occurred 210 ms after MCx spikes. **C**, Population data of paired VAVL-MCx recordings. There was no significant difference between control rats ($n = 25$) and the lesioned hemisphere ($n = 24$)

with respect to the proportions of VAVL-MCx spike train pairs with correlated activity (top) or the timing of VAVL firing relative to MCx (bottom).

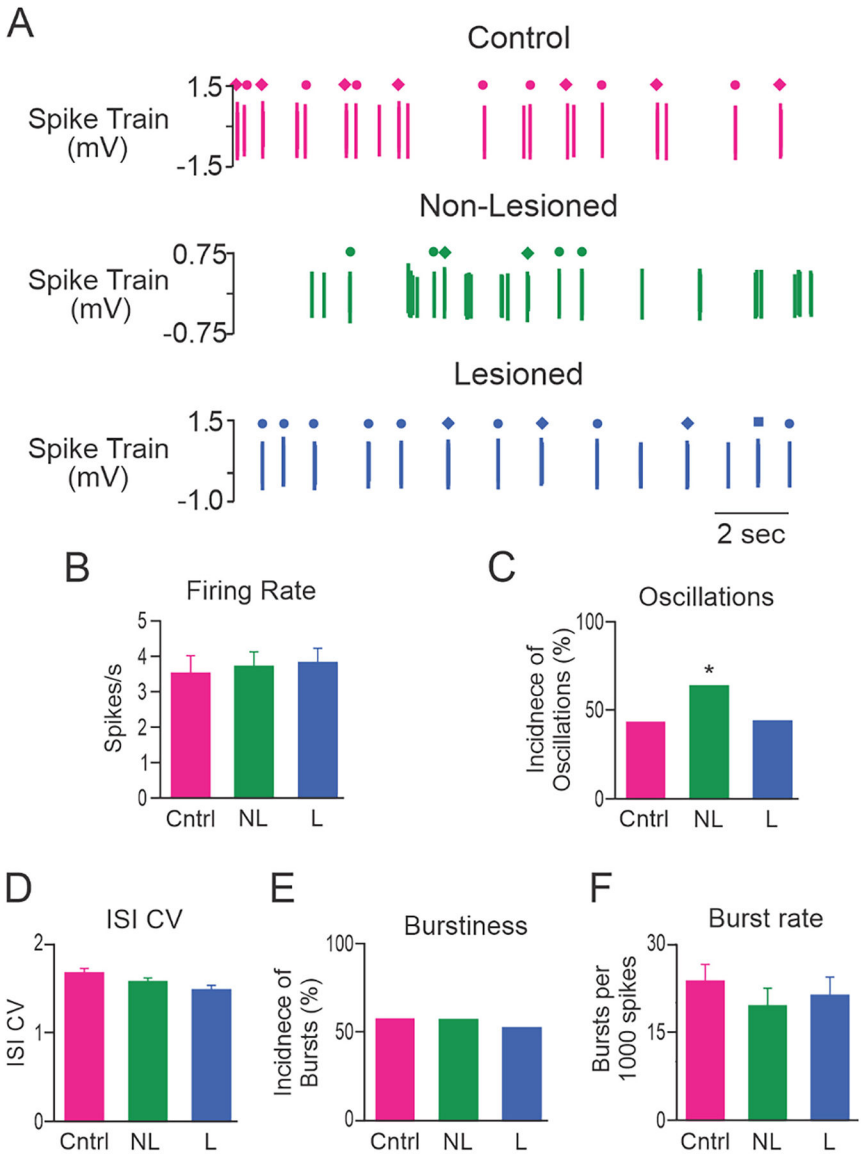

Fig. 6.

Characteristics of VAVL spike trains. **A**, VAVL spike trains from control (Cntrl; top, red) rats, and non-lesioned (NL; middle, green) and dopamine lesioned (L; bottom, blue) hemispheres. Firing rates of these 3 neurons were 2.8, 2.6 and 1.8 spikes/s, respectively. Dots, diamonds and squares above spikes indicate the position of LTS bursts containing 2, 3 and 4 spikes, respectively. **B**, Mean firing rate. **C**, Incidence of spike trains with significant 0.3–2.5 Hz oscillatory activity. **D**, Mean ISI CV. **E**, Incidence of bursty spike trains. **F**, Burst rate. Firing rate and spike train oscillatory activity was not significantly different between control and dopamine lesioned hemispheres. However, significantly more spike trains in the non-lesioned hemisphere had oscillatory activity than control or lesioned hemispheres. * Significant difference of $p < 0.05$ compared to control rats. $n = 63$ cells from 10 Cntrl rats, $n = 60$ from 15 NL hemispheres and $n = 66$ from 17 L hemispheres.

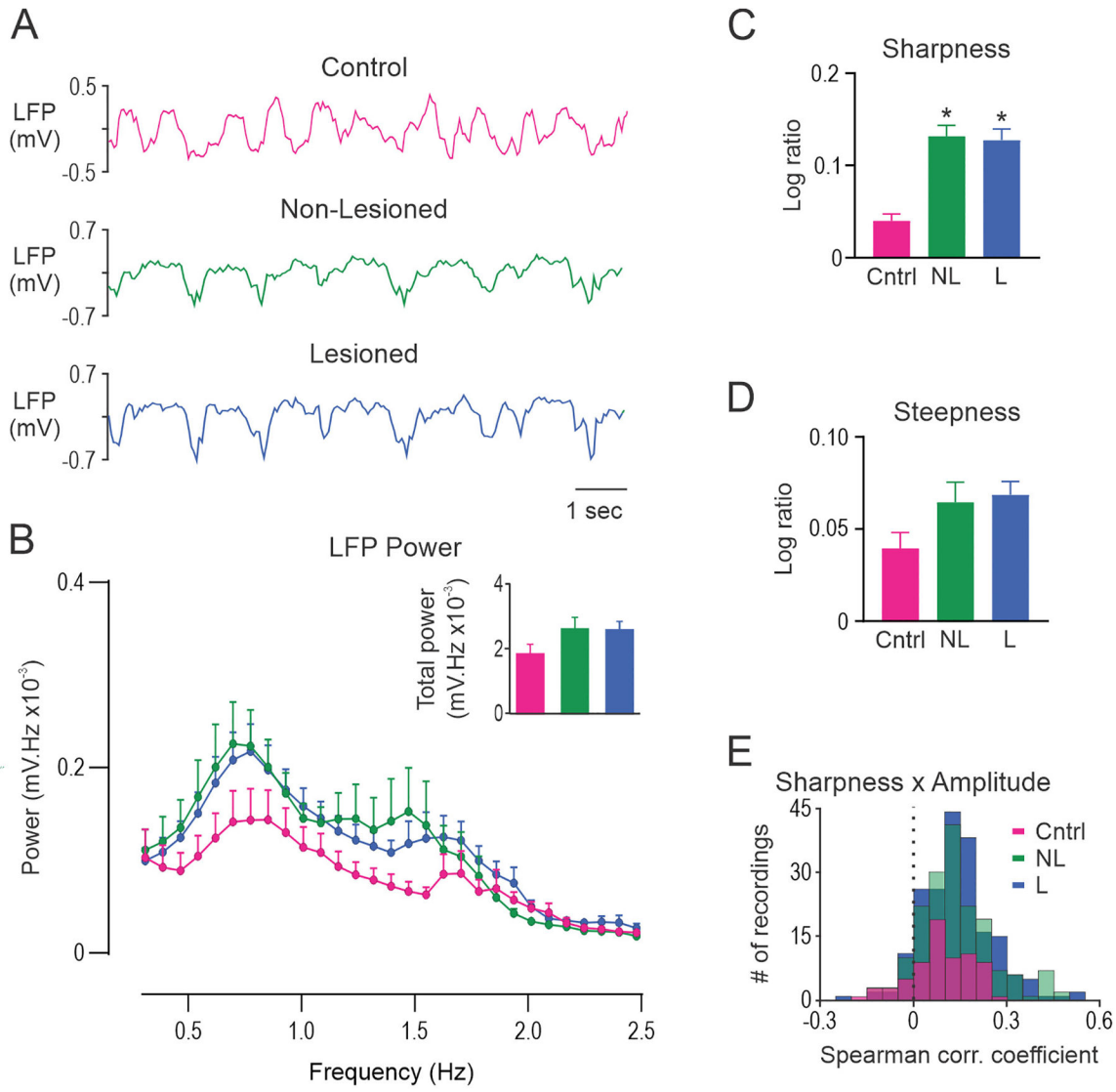

Fig. 7.

Unilateral dopamine lesion alters the shape of slow-wave oscillations in VAVL thalamus but does not alter FFT power. **A**, Representative segments of VAVL LFP activity in control rats (Cntrl; top, red), and non-lesioned (NL; middle, green) and dopamine lesioned (L; bottom, blue) hemispheres of unilateral 6-OHDA lesioned rats. **B**, FFT power spectral density over the 0.3–2.5 Hz range. Total power was not different between the groups (inset). **C**, Sharpness ratio was significantly larger in non-lesioned and lesioned hemispheres than in control rats. **D**, Steepness ratio did not differ between control rats, and non-lesioned and lesioned hemispheres. **E**, On average, there was a positive correlation between cycle sharpness ratio and amplitude for LFPs recorded from control rats and both hemispheres in lesioned rats. * Significant difference of $p < 0.05$ compared to control rats. LFP's recorded from different electrode tracks were averaged to give a single data point for each rat. $n = 13$ Cntrl, $n = 22$ NL and $n = 34$ L.

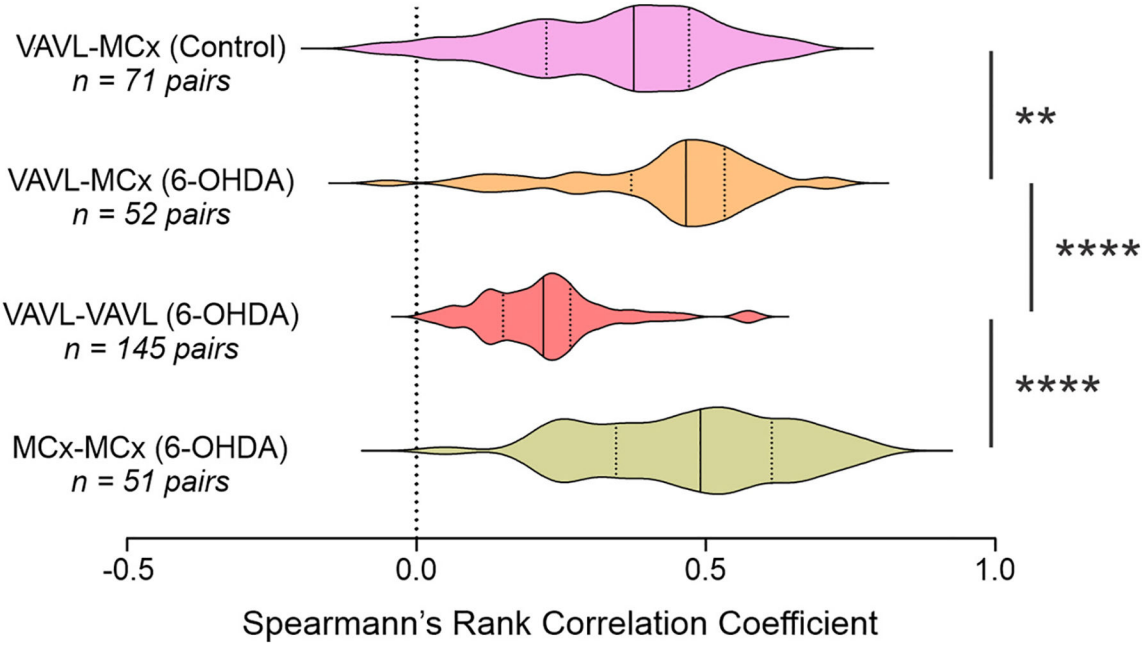

Fig. 8.

Cycle-by-cycle computation of sharpness ratio in paired recordings. Sharpness asymmetry was positively correlated between the ipsilateral VAVL and MCx in control and lesioned rats and between lesioned and non-lesioned hemispheres in MCx or VAVL in lesioned rats. Correlation coefficients were larger for VAVL-MCx paired recordings in lesioned than control rats and for MCx-MCx than VAVL-VAVL paired recordings in lesioned rats. ** and **** indicate significant difference of $p < 0.01$ and $p < 0.0001$, respectively, for groups indicated.

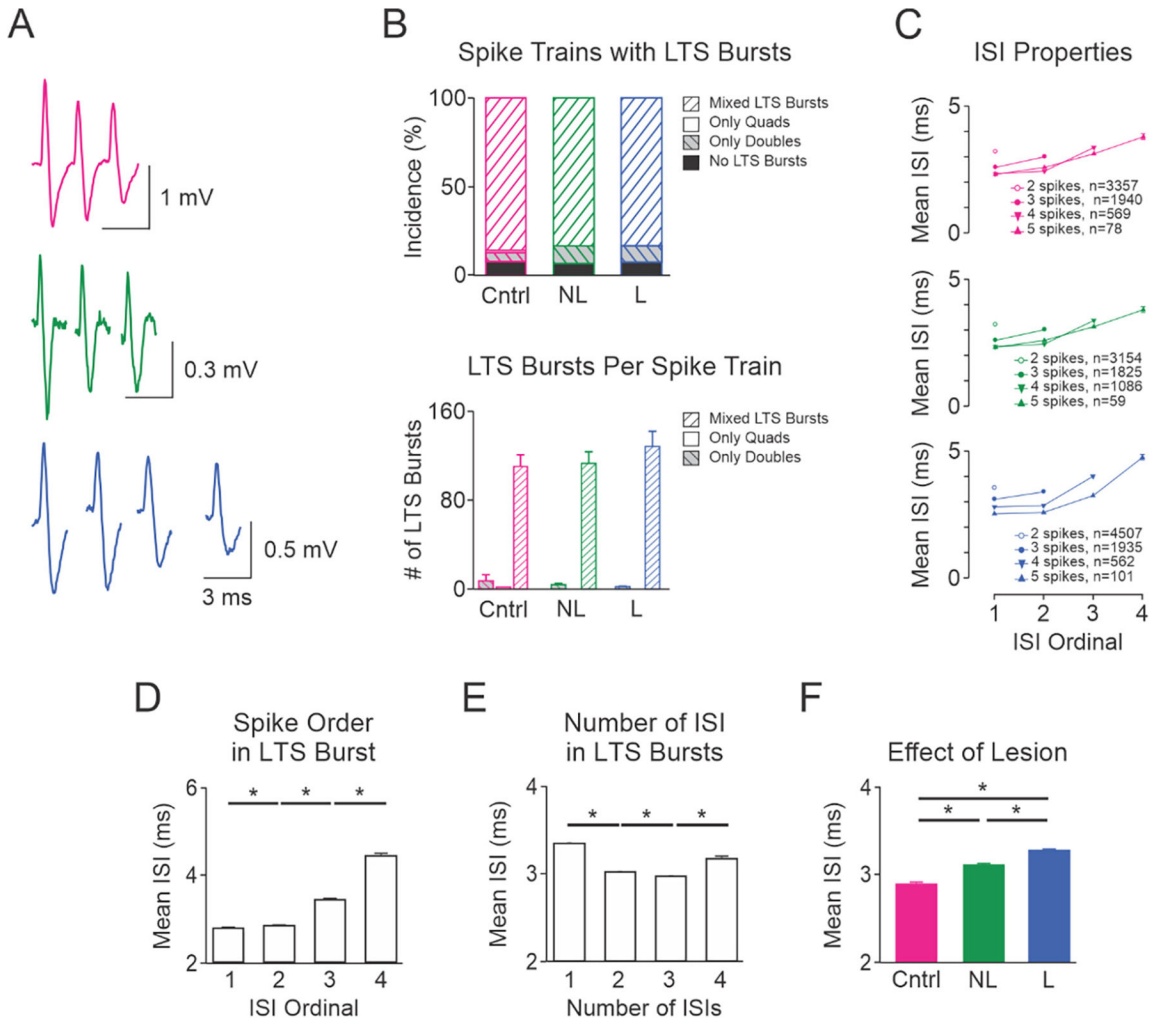

Fig. 9.

Characteristics and timing of VAVL spikes in LTS bursts. **A**, Example LTS bursts in control rats (triplet; top, red) and non-lesioned (triplet; middle, green) and dopamine lesioned (quad; bottom, blue) hemispheres of unilateral 6-OHDA lesioned rats. **B**, Upper bar graph shows the proportion of spike trains that had no LTS bursts, contained only doublets or quadruplets, or contained a combination of 2–8 spikes in LTS bursts (mixed LTS bursts). Dopamine cell lesion did not affect the proportion of spike trains that contained no LTS bursts, only doublets, only quadruplets or mixed types of LTS bursts. Lower bar graph shows that dopamine cell lesion did not affect the mean number of LTS bursts in spike trains that contained only doublets, only quadruplets or mixed types of LTS bursts. **C**, Mean interspike intervals (ISI) in LTS bursts in control (top), non-lesioned (middle) and lesioned (bottom) hemispheres. The numbers of LTS bursts containing doublets, triplets, quadruplets and quintuplets are shown within each graph. Bar graphs in the lower panel (**D**–**F**) show how mean ISI is influenced by the position of the ISI in LTS bursts (**D**), number of ISIs in LTS bursts (**E**) and lesion (**F**). A 3 factor ANOVA revealed that all single factors (lesion, number of ISIs and position of ISIs) were statistically significant ($p = 0.001$). Post-hoc analysis revealed that ISI durations differed significantly based on: the position of ISIs in

the LTS bursts (D), the number of ISIs (E), and hemisphere (F). All two factor interactions were significant (p = 0.001). There were no significant interactions between all 3 factors on ISIs in LTS bursts. *Significant difference of $p < 0.05$. Abbreviations: Cntrl control rats, NL non-lesioned hemisphere, L lesioned hemisphere.